International Geology Review

ISSN: 0020-6814 (Print) 1938-2839 (Online) Journal homepage: https://www.tandfonline.com/loi/tigr20

The Jurassic tourmaline–garnet–beryl semi-gemstone province in the Sanandaj–Sirjan Zone, western Iran

Fatemeh Nouri, Robert J. Stern & Hossein Azizi

To cite this article: Fatemeh Nouri, Robert J. Stern & Hossein Azizi (2018): The Jurassic tourmaline–garnet–beryl semi-gemstone province in the Sanandaj–Sirjan Zone, western Iran, International Geology Review

To link to this article: https://doi.org/10.1080/00206814.2018.1539927

Published online: 01 Nov 2018.

INTERNATIONAL GEOLOGY REVIEW
https://doi.org/10.1080/00206814.2018.1539927

Taylor & Francis
Taylor & Francis Group

ARTICLE

The Jurassic tourmaline–garnet–beryl semi-gemstone province in the Sanandaj–Sirjan Zone, western Iran

Fatemeh Nouri[a], Robert J. Stern[b] and Hossein Azizi [c]

[a]Geology Department, Faculty of Basic Sciences, Tarbiat Modares University, Tehran, Iran; [b]Geosciences Department, University of Texas at Dallas, Richardson, TX, USA; [c]Department of Mining, Faculty of Engineering, University of Kurdistan, Sanandaj, Iran

ABSTRACT

Deposits of semi-gemstones tourmaline, beryl, and garnet associated with Jurassic granites are found in the northern Sanandaj–Sirjan Zone (SaSZ) of western Iran, defining a belt that can be traced for about 400 km. Granitic magmas strongly interacted with or were derived from melts of continental crust and/or sediments. Based on morphologies, size, mineral assemblage, and contact relationships with host granite and associated metamorphic aureoles, these deposits are categorized into six types: (1) garnet in skarns, (2) tourmaline, beryl, and garnet in pegmatite and aplitic dikes, (3) disseminations and patches of tourmaline in leucogranites, (4) quartz-tourmaline veins in granite, (5) tourmaline and garnet in metamorphic aureoles, and (6) tourmaline orbicules in aplite. Tourmalines are mostly schorl and dravite, and garnets are mostly almandine, spessartine, and grossular. Tourmaline, beryl, and garnet from pegmatites in the contact aureole of Jurassic granites reflect segregations of Be, B, Mn, and Al bearing melts from the Jurassic peraluminous granites. Quartz-tourmaline veins and hydrothermal garnets in skarns reflect fluids exsolved from the surrounding metasediment and pegmatite melt. In contrast, tourmaline patches and orbicules developed from boron-rich aqueous fluids exsolved from cooling granitic magma. Distribution of semi-gemstones in the SaSZ shows that these are mostly related to pegmatites associated with Jurassic granitic intrusions. Mineral equilibrium considerations indicate that SaSZ semi-gemstones crystallized at P = 3.5–7.5 kbar (11.5–25 km deep) and temperatures of 550–650°C. SaSZ pegmatites fall in the muscovite (MS) and MS-rare element classes. They are Lithium Cesium Tantalum (LCT)-type pegmatites. Fluids responsible for gem mineralization were exsolved from cooling granite bodies and released by metamorphosed sediments. Further studies are needed to better understand the northern Sanandaj–Sirjan tourmaline–garnet–beryl semi-gemstone Province.

ARTICLE HISTORY
Received 5 August 2018
Accepted 20 October 2018

KEYWORDS
Semi-gemstone; pegmatite; tourmaline; garnet; beryl; Sanandaj–Sirjan Zone; Iran

1. Introduction

The geology of Iran reflects diverse tectonic events and magmatic episodes (Stöcklin 1968; Berberian and Berberian 1981; Berberian *et al*. 1982; Alavi 1994; Mohajjel and Fergusson 2000; Mohajjel *et al*. 2003; Golonka 2004; Ghasemi and Talbot 2006; Davoudian *et al*. 2008; Azizi *et al*. 2011; 2017; Chiu *et al*. 2013; Moghadam *et al*. 2016); consequently, there are a wide range of lithologies and minerals, including semi-gemstones. Iranian people have mined and used gemstones and semi-gemstones throughout its >7000-year history. In ancient times, before humans learned how to cut hard minerals, rough gemstones and semi-gemstones were valued for their magical properties in addition to their material value and possessing them was considered lucky (Ghorbani 2003).

The jewellery and gem industry in Iran has a history of several thousand years, and Iranian interest in gems and jewellery is deeply rooted in this history (Meen and Tushigham 1968; Ghorbani 2003). About 200 regions in Iran are identified as gemstone and semi-gemstone regions (Ghorbani 2003; Nekouvaght Tak and Bazargani-Guilani 2009; Tahmasbi *et al*. 2009, 2017; Sheikhi *et al*. 2012; Salami *et al*. 2013; Khodakarami Fard *et al*. 2014; Mansouri Esfahani and Khalili 2014; Tahmasbi 2014; Alipour *et al*. 2015; Ahmadi Khalaji *et al*. 2016). Iran has diverse gemstones and semi-gemstones such as opal, turquoise, beryl, fluorite, kyanite, garnet, agate, peridot, and jasper (Ghorbani 2003; Kievlenko 2003; Groat and Laurs 2009, 2014; Huong *et al*. 2012; Clark *et al*. 2016). But realizing this potential is hampered because of the lack of systematic scientific study beyond studies of individual deposits (Ghorbani 2003; Nekouvaght Tak and Bazargani-Guilani 2009; Tahmasbi *et al*. 2009, 2017; Sheikhi *et al*. 2012; Salami *et al*. 2013; Khodakarami Fard *et al*. 2014; Mansouri

CONTACT Fatemeh Nouri f.nourisandiani@gmail.com Geology Department, Faculty of Basic Sciences, Tarbiat Modares University, Tehran, Iran

Esfahani and Khalili 2014; Tahmasbi 2014; Alipour *et al*. 2015; Ahmadi Khalaji *et al*. 2016). What is especially needed is a better understanding of related deposits that can be considered together as manifestations of gemstone and semi-gemstone – forming episodes that can be defined in space and time. Similar episodes affecting similar rocks under similar conditions are likely to produce similar mineral suites, making it useful to consider defining gemstone and semi-gemstone provinces wherever possible and interpreting these as gemstone and semi-gemstone-forming systems. Such an effort requires an interdisciplinary approach involving field geology, mineralogy, geochemistry, geochronology, and isotopic studies. Similar approaches have proved to be useful for systematic study of hydrocarbons (hydrocarbon provinces) and metals (metallogenic provinces) (Worden *et al*. 2000; Somarin 2004; Bordenave and Hegre 2005; Zhou *et al*. 2007; Bernard *et al*. 2012).

Here we use the geoprovince approach to study semi-gemstones of the Sanandaj–Sirjan zone (SaSZ). The SaSZ is a well-defined geologic terrane that experienced pervasive magmatism, metamorphism, and deformation, and has abundant pegmatites, metamorphic aureoles, and migmatites, environments that sometimes produce pockets of semi-gemstones. There are many short reports on SaSZ deposits of tourmaline (Nezam abad, Haji abad, Astaneh, and Mangavi), garnet (Boroujerd, Molataleb, Abaru, Kamari-Zaman Abad, and Seranjik), and beryl (Ebrahim Atar and Kamari-Zaman Abad) (Nekouvaght Tak and Bazargani-Guilani 2009; Tahmasbi *et al*. 2009; Sheikhi *et al*. 2012; Salami *et al*. 2013; Khodakarami Fard *et al*. 2014; Mansouri Esfahani and Khalili 2014; Tahmasbi 2014; Ahmadi Khalaji *et al*. 2016), but there is no systematic overview of SaSZ semi-gemstone deposits. This study aims to help overcome this shortcoming by summarizing what is known about semi-gemstones of the SaSZ of Southwest Iran, with special emphasis on its tourmaline, beryl, and garnet deposits.

2. Geological setting

The SaSZ is a distinctive terrane that is 50–150 km wide, 800 km long and trends southeast–northwest across Southwest Iran (Figure 1). The SaSZ has been part of the Iran active margin since Middle Jurassic time (Stöcklin 1968; Berberian and Berberian 1981; Berberian *et al*. 1982; Mohajjel *et al*. 2003; Golonka 2004; Ghasemi and Talbot 2006; Davoudian *et al*. 2008; Nadimi and Konon 2012) and helps define the southwest margin of the Iranian microcontinent (Stöcklin 1968; Berberian and Berberian 1981; Mohajjel *et al*. 2003; Hassanzadeh *et al*. 2008; Azizi *et al*. 2016). A variety of marine sediments were deposited in Palaeozoic and Mesozoic time. Igneous activity was concentrated in Jurassic time (Azizi and Moinevaziri 2009; Mahmoudi *et al*. 2011; Azizi and Asahara 2013; Mohajjel and Fergusson 2014). SaSZ sedimentary rocks are regionally metamorphosed, especially around Jurassic plutons (Berberian and Berberian 1981; Sepahi and Athari 2006; Ahmadi-Khalaji *et al*. 2007; Sepahi 2007; Azizi *et al*. 2011; Maanijou *et al*. 2011; Aliani *et al*. 2012; Azizi and Asahara 2013; Yajam *et al*. 2015; Deevsalar *et al*. 2017). SaSZ basement consists of Ediacaran-Cambrian (Cadomian) igneous and metamorphic rocks (Stöcklin 1968; Berberian and Berberian 1981; Berberian *et al*. 1982; Mohajjel *et al*. 2003; Golonka 2004; Ghasemi and Talbot 2006; Davoudian *et al*. 2008; Hassanzadeh *et al*. 2008; Malek-Mahmoudi *et al*. 2017; Shabanian *et al*. 2017). Codomian (~550 Ma) basement is exposed in the northern SaSZ (Moghadam *et al*. 2015, 2016; Honarmand *et al*. 2017; Shabanian *et al*. 2017) but Jurassic metamorphic rocks cut by Late Jurassic granitoids make up most outcrops (Berberian *et al*. 1982; Baharifar *et al*. 2004; Esmaeily *et al*. 2005; Sepahi and Athari 2006; Arvin *et al*. 2007; Mazhari *et al*. 2009; Shahbazi *et al*. 2010, 2014; Azizi and Asahara 2013; Azizi *et al*. 2011, 2015a; b, 2016; Zhang *et al*. 2018). Major plutonic rocks of this area are granites, diorites, and gabbros which are intruded by aplite-pegmatitic and silicic veins. Both I-type and S-type granitic rocks are encountered.

The Jurassic volcano-sedimentary complex is an important part of the SaSZ. Jurassic volcanics and volcaniclastics are associated with marble, black shale, pelite, psammite, mafic volcanics, calc-pelite, and calc-silicate rocks. Pelitic rocks are the most abundant lithology. The pelitic sequence has been variably metamorphosed to slate, phyllite, mica schist, garnet schist, garnet andalusite schist, garnet staurolite schists, cordierite hornfels, mica hornfels, garnet hornfels, and garnet andalusite hornfels. Metamorphic rocks were overprinted by dynamic deformation (Mohajjel *et al*. 2003; Baharifar *et al*. 2004; Davoudian *et al*. 2008). Metamorphic rocks are locally unconformably overlain by Cretaceous marble (Eftekharnejad 1981; Kazmin *et al*. 1986; Alavi 1994; Hosseiny 1999; Baharifar *et al*. 2004).

3. Semi-gemstone districts in the SaSZ

Table 1 lists and Figure 1(b) shows the main SaSZ semi-gemstone deposits, from northwest to southeast. Below we discuss these deposits and their host rocks based on geographic location. We subdivide the SaSZ semi-gemstone province into three districts, each on the order of

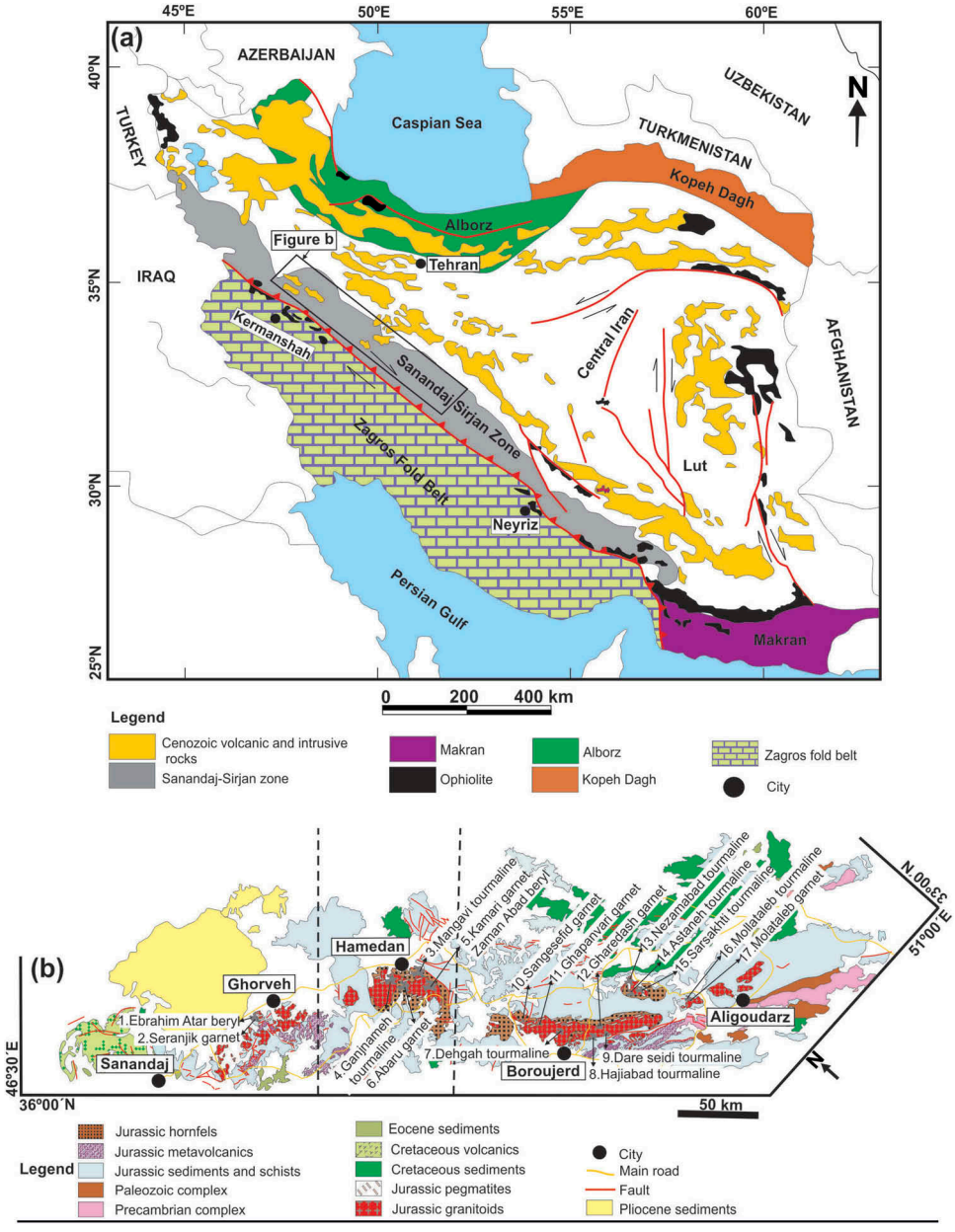

Figure 1. (a) Simplified geological map of Iran (modified from Stöcklin 1968). (b) Simplified geology map of northern part of Sanandaj–Sirjan Zone which shows the location of semi-gemstone deposits and their host rocks (modified from Bayati et al., 2017).

50–200 km across. From northwest to southeast, the three SaSZ semi-gemstone districts are (1) Ghorveh, (2) Hamedan, and (3) Boroujerd (Figure 1(b)). These are further outlined below.

3.1. Ghorveh semi-gemstone district

The Ghorveh semi-gemstone district is the most important one in the SaSZ and consists of two principal semi-gemstone areas: Ebrahim Atar S-type pegmatite and Seranjic skarn (Figure 1(b)). These are located near the Moshirabad (I-type granite) and Ghalaylan (A-type granite) plutons (Azizi *et al*. 2011, 2015b, 2016; Mahmoudi *et al*. 2011; Salami *et al*. 2013; Yajam *et al*. 2015). These deposits are associated with the Jurassic Hamedan-Ghorveh metamorphic complex, a suite of slate, phyllite, schist, marble, and quartzite that is interbedded with submarine metavolcanic rocks and associated with abundant pegmatites (Hosseiny 1999; Baharifar *et al*. 2004; Azizi and Asahara 2013). Outcrops of the Moshirabad granitoid define a sigmoidal form of medium- to coarse-grained granites (Figure 2(a)) and metaluminous to peraluminous granitoids (Figure 2(b)) (Yajam *et al*. 2015). The 157 Ma Moshirabad I-type granite plots in the volcanic arc granite (VAG) field due to their low

Table 1. Location of semi-gemstone deposits and their host rocks.

District	Number (Figure 1)	Area	Semi-gem	Colour	Feature
Ghorveh	1	Ebrahim Atar	Beryl	Green, blue	1. Vein
	2	Seranjic	Garnet	Brown, green	1. Vein, 2. aggregate
Hamedan	3	Mangavi	Tourmaline	Black	1. Pegmatite
	4	Ganjnameh	Tourmaline	Black	1. Pegmatite
	5	Kamari	Garnet	Brown, red	1. Spot, 2. aggregate
	6	Abaru	Garnet	Brown, red	1. Spot, 2. aggregate
Boroujerd	7	Dehgah	Tourmaline	Black to green	1. Nodule or lobar
	8	Haji-abad	Tourmaline	Black	1. Pegmatite, 3. quartz-tourmaline vein, 4. metamorphic halo
	9	Dare Seidi	Tourmaline	Black to green	1. Vein, 2. stringer
	10	Sangesefid	Garnet	Light reddish	1. Pegmatite
	11	Ghapanvari	Garnet		1. Pegmatite
	12	Gharedash	Garnet		1. Pegmatite
	13	Nezam abad	Tourmaline	Black	1. Aplitic dike, 2. hydrothermal vein
	14	Astaneh	Tourmaline	Black	1. Nodule, 2. stratiform toumalinite
	15	Sarsakhti	Tourmaline	Black to green	1. Nodule or lobar
	16	Molataleb	Tourmaline	Black	1. Pegmatite
	17		Garnet	Brown, green	1. Lobar, 2. spot

Source	References	Host rock	Other minerals	Age (Ma)	Method
Magmatic origin	Salami *et al*. (2013)	Pegmatite granite	Quartz, alkali feldspar, muscovite, biotite, garnet, and alanite	134 ± 29	Sm-Nd
Metamorphic and metasomatic origins	Sheikhi *et al*. (2012)	Skarn and hornfels that surrounded by granites	Clinopyroxene, garnet, vesuvianite, wollastonite, titanite, and epidote	160 ± 2	U-Pb
Metamorphic origin	Ahmadi Khalaji and Tahmasbi (2015)	Leucogranites and granodiorites surronded by hornfels and Jurassic phylliteschist	Quartz, alkali feldspar, plagioclase, muscovite, biotite, garnet, apatite, and zircon	163 ± 0.88	U-Pb
Magmatic origin	Ahmadi Khalaji and Tahmasbi (2015)	Pegmatite veins that surrounded by granidiorite, hornfles, and Jurassic phylites			
Metamorphic origin	Ahmadi Khalaji and Tahmasbi (2015)	Schist and hornfels that surrounded by granites			
Magmatic origin	Ahmadi Khalaji and Tahmasbi (2015)	Pegmatite veins that surrounded by granidiorite, hornfles, and Jurassic phylites			
Magmatic origin	Tahmasbi (2014)	Aplitic dikes that surrounded by granidiorite, hornfles and Jurassic phylites	Quartz, alkali feldspar, muscovite, and plagioclase	168 ± 0.85	U-Pb
Magmatic, metamorphic, and hydrothermal origins	Khodakarami Fard *et al*. (2014)	Leucogranitic granite surronded by hornfels and Jurassic phyllite-schist	Quartz, alkali feldspar, muscovite, plagioclase, amphibole, epidote, zircon, and alanite		
Hydrothermal origin	Gholami and Mokhtari ()	Granite and granidiorite surrounded by Jurassic phylites and schists	Quartz		

(*Continued*)

Table 1. (Continued).

District	Number (Figure 1)	Area	Semi-gem	Colour	Feature
Magmatic origin	Rahmani Javanmard *et al*. (2018)	Pegmatite granite	Quartz, alkali feldspar, muscovite, andulusite, tourmaline, zircon, and flourapatite	170 ± 1.5	U-Pb
Magmatic origin	Rahmani Javanmard *et al*. (2018)	Pegmatite granite			
Magmatic origin	Rahmani Javanmard *et al*. (2018)	Pegmatite granite			
Magmatic and hydrothermal origin	Nekouvaght Tak and Bazargani-Guilani (2009)	Quartz diorite and granidiorite surrounded by hornfles and Jurassic phylites	Plagioclase, hornblende, biotite, quartz, titanite, and zircon	167 ± 1.0	U-Pb
Hydrothermal fluids for nodules and metasomatism at the contact of plutonicand hornfels	Tahmasbi *et al*. (2009)	Monzogranite surrounded by Jurassic phylites and schists	Muscovite, biotite, quartz, plagioclase, and alkali feldspar	169 ± 1.0	U-Pb
Magmatic origin and reaction with fluids derived of metapelitic host rock	Tahmasbi (2014)	Monzo granite	Quartz, alkali feldspar, plagioclase, zircon, and apatite	169 ± 1.0	U-Pb
Metasomatism at the contact of intrusive body and pelitic hornfels	Mansouri Esfahani and Khalili (2014)	Pegmatitic veins that surrounded by micaseous granodiorite and metapelites	Quartz, alkali feldspar, plagioclase, zircon, and apatite	165 ± 5	U-Pb
Magmatic origin	Mansouri Esfahani and Khalili (2014)	Two mica granite and metapelitic rocks		165 ± 5	U-Pb

Latitude	Longitude	Temperature	Pressure	References
35°08′	47°40′			
35°09′	47°47′	450–587°C	<3 kbar	Sheikhi *et al*. (2012)
34°38′	48°44′			
34°45′	48°24′			
34°36′	48°43′	568–586°C	4.3 ± 0.5 kbar	Baharifar (1997)
34°41′	48°32′			
33°45′	48°50′			
33°40′	49°14′			
33°55′	48°49′			
33°46′	49°00′			
33°53′	48°55′			
33°59′	48°48′			
33°40′	49°16′			
33°59′	49°17′			
33°41′	49°21′			
33°35′	49°35′			
33°35′	49°35′			

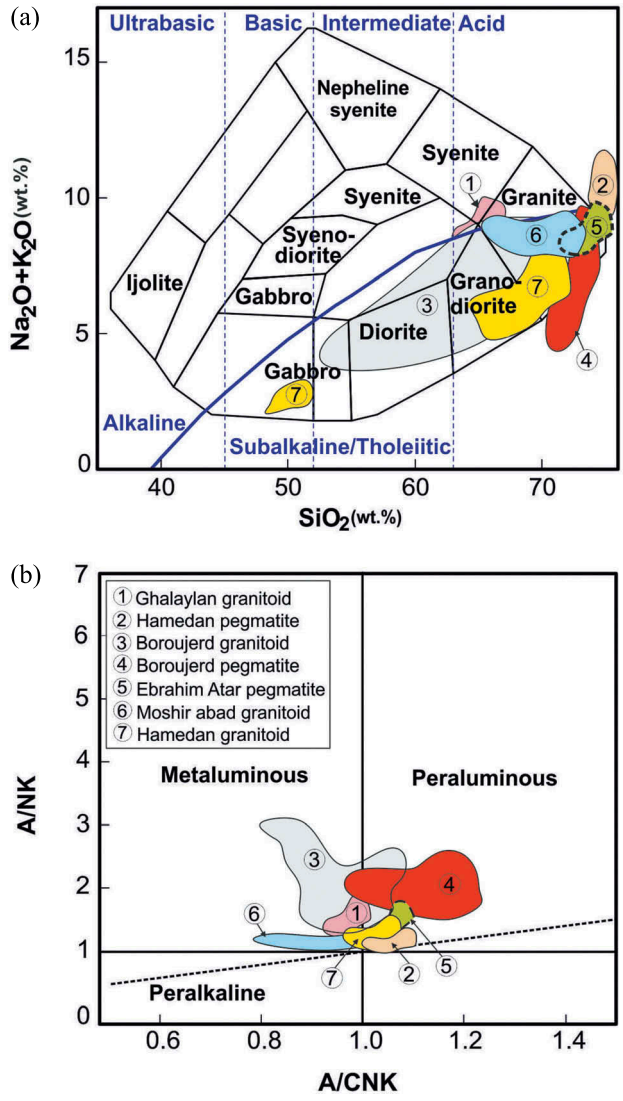

Figure 2. Geochemistry of SaSZ Jurassic granitic and pegmatitic rocks. (a) Total alkalis *versus* SiO_2 diagram (Cox *et al*. 1979). (b) A/NK (molar $Al_2O_3/(Na_2O + K_2O)$ *versus* A/CNK (molar $Al_2O_3/(CaO + Na_2O + K_2O)$ diagram (Maniar and Piccoli 1989). Data for Ghalaylan, Moshirabad, Ebrahim Atar, Hamedan, and Boroujerd granitoids from Azizi *et al*. (2015b), Azizi *et al*. (2016), Yajam *et al*. (2015), Shahbazi *et al*. (2010), (2014), Ahmadi-Khalaji *et al*. (2007), Tahmasbi *et al*. (2010), Esna-Ashari *et al*. (2012), Rahmani Javanmard *et al*. (2018), Sepahi *et al*. (2018).

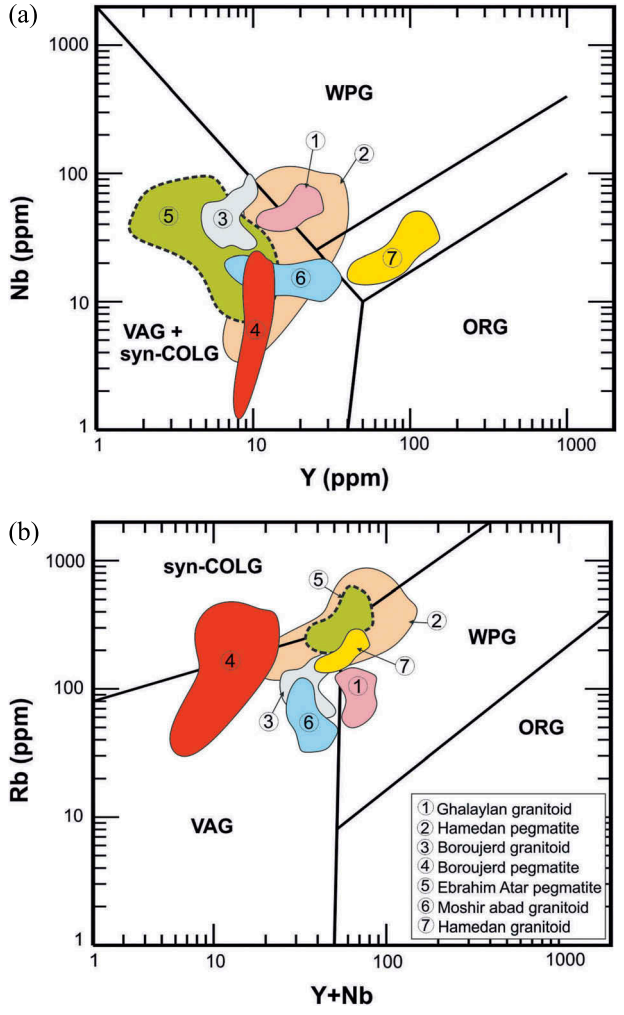

Figure 3. (a, b) Pearce *et al*. (1984) discriminant diagrams for granitoids and pegmatites from Ghorveh, Hamedan, and Boroujerd in SaSZ. Data for Ghalaylan, Moshirabad, Ebrahim Atar, Hamedan, and Boroujerd granitoids from Azizi *et al*. (2015b), Azizi *et al*. (2016), Yajam *et al*. (2015), Shahbazi *et al*. (2010), (2014), Ahmadi-Khalaji *et al*. (2007), Tahmasbi *et al*. (2010), Esna-Ashari *et al*. (2012), Rahmani Javanmard *et al*. (2018), Sepahi *et al*. (2018).

concentrations of Nb and Ta (Figures 3 and 4(a)) (Yajam *et al*. 2015). The Ghalaylan granite differs from other Jurassic intrusions in the Ghorveh area, which have moderate contents of SiO_2 (62–68 wt%; Figure 2(a)) and are mainly metaluminous to peraluminous (Figure 2(b)). Ghalaylan is A-type, ferroan and has a composition similar to adakite and tonalite–trondhjemite–granodiorite (Azizi *et al*. 2015b). In the tectonic discrimination diagram of Pearce *et al*. (1984), the Ghalaylan granitoid plots within the transitional area between the field of VAG and within-plate granite (Figure 3). It has a zircon U-Pb age indicating an age of 157 Ma (Figure 4(a)) (Azizi *et al*. 2015b).

The Ebrahim-Atar pegmatite contains alkali feldspar, quartz, plagioclase, muscovite (MS), and biotite (Salami *et al*. 2014; Azizi *et al*. 2016). It is characterized by high SiO_2 (72.81 wt%) (Figure 2(a)) and Rb (140–440 ppm) contents and low contents of MgO (<0.12 wt%), Fe_2O_3 (<0.68 wt%), Sr (mainly <20 ppm), Ba (<57 ppm), Zr (10–53 ppm), and rare earth elements (REE; 3.88–94.9 ppm; mean = 21.2 ppm). Chemical compositions and mineral parageneses show that the Ebrahim Atar pegmatite is peraluminous and was generated by partial melting of

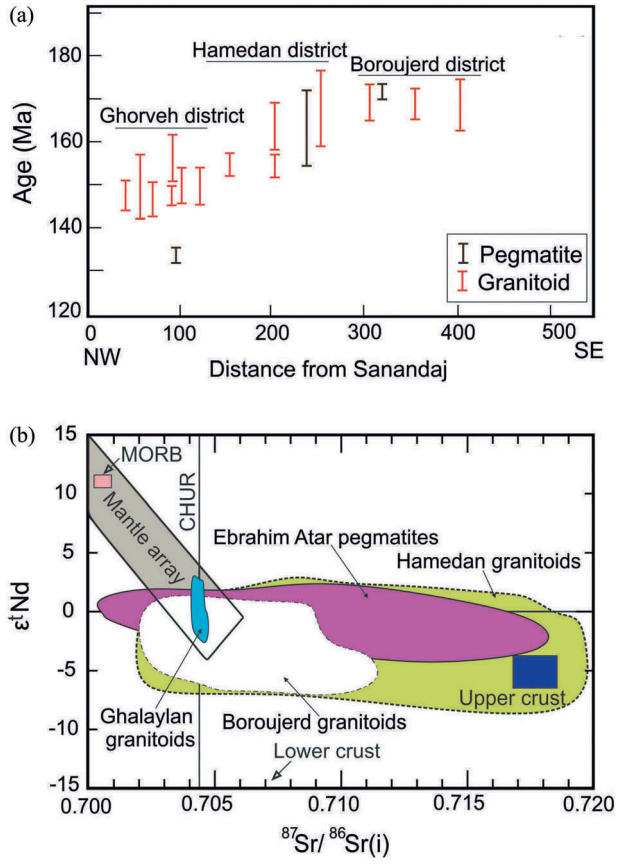

Figure 4. (a) Simplified age diagram for granitoids and pegmatites from N-SaSZ. Age data for Ghorveh from Azizi *et al*. (2011), Azizi *et al*. (2015a), (2015b), (2016), Mahmoudi *et al*. (2011) and Yajam *et al*. (2015), Hamedan from Shahbazi *et al*. (2010), Deevsalar *et al*. (2017), and Sepahi *et al*. (2018). Boroujerd from Ahmadi-Khalaji *et al*. (2007), Esna-Ashari *et al*. (2012), Shakerardakani *et al*. (2015), and Deevsalar *et al*. (2017). (b) Sr and Nd isotopic data for granitic rocks from Ghalayan, Hamedan, Ebrahim Atar, and Boroujerd (Sr and Nd isotope data from Ahmadi-Khalaji *et al*. (2007), Shahbazi *et al*. (2010), Tahmasbi *et al*. (2010), Esna-Ashari *et al*. (2012), Azizi *et al*. (2015b), (2016)). These granitic rocks have a strong crustal component, derived from continental crust, metasediments, or both.

siliciclastic to pelitic rocks (Figure 2(b)); it is an S-type leucogranite pegmatite (Azizi *et al*. 2016). The pegmatite and its associated granite differ from other SaSZ Jurassic granites. The initial Sr-Nd isotopic compositions of Ebrahim Atar granites are pointedly different from those of Ghalaylan and Moshirabad granites have positive $\varepsilon Nd_{(t)}$ values, whereas Ebrahim Atar granites display negative $\varepsilon Nd_{(t)}$ values. A further difference is that Ghalaylan granite is post-tectonic; moreover, the low REE content infers that partial melting produced the Ebrahim Atar granites from rocks with low REE content, such as siliciclastic or metapelitic rocks (Azizi *et al*. 2015b, 2016). In the Pearce *et al*. (1984) diagram, most Ebrahim-Atar samples plot in the field for VAG but extend into fields for syn-collision and within-plate granite (Figure 3).

Deposits of beryl (Salami *et al*. 2013), tourmaline, and garnet (Sheikhi *et al*. 2012) of this district have magmatic and metasomatic origins, including the Ebrahim Atar beryl and Seranjic garnet deposits (Sheikhi *et al*. 2012; Salami *et al*. 2013) (Table 1). Rb-Sr whole rock and Sm-Nd dating indicate that the Ebrahim Atar pegmatite crystallized at 134 ± 29 Ma (Figure 4(a)) (Azizi *et al*. 2016), significantly younger than the ages of the Moshirabad and Ghalaylan plutons. The $^{87}Sr/^{86}Sr$ (i) = 0.7081 and $\varepsilon Nd_{(t)}$ values range from −5.8 to −1.6, indicating the involvement of older continental crust and/or sediments (Azizi *et al*. 2016) (Figure 4(b)).

3.2. Hamedan semi-gemstone district

The Hamedan semi-gemstone district is located around the Alvand plutonic complex and deposits are concentrated in four areas: Mangavi, Ganjnameh, Kamari-Zaman Abad, and Abaru (Figure 1(b)). These deposits are mostly of magmatic and metamorphic origins. The Alvand pluton is dominated by gabbro and coarse porphyritic granite (Figure 2(a)) with metaluminous to peraluminous compositions (Figure 2(b)) which intruded 164–162 Ma ago (Figure 4) (Shahbazi *et al*. 2010). In the discrimination diagram of Pearce *et al*. (1984), all Hamedan granitoids plot close to fields for within-plate granite and VAG. Aplitic and pegmatite rocks cross-cut plutonic and metamorphic rocks in the Hamedan-Alvand region. Gabbroic rocks are calc-alkaline with low initial $^{87}Sr/^{86}Sr$ ratios (0.7023–0.7037) and positive $\varepsilon Nd_{(t)}$ = +2.9 to +3.3. In contrast, the granites show high to low K calc-alkaline signatures with A-type affinity and have intermediate to high initial $^{87}Sr/^{86}Sr$ (0.707–0.714) and negative $\varepsilon Nd_{(t)}$ = −1.0 to −3.4 (Figure 4(b)) (Shahbazi *et al*. 2010), showing evidence for involvement of sediments or older crust. Alvand granites intrude Triassic-Jurassic phyllites, schists, metavolcanics, and dolomitic limestone (Baharifar *et al*. 2004; Shahbazi *et al*. 2010, 2014). Mohajjel and Izadikian (2007) reported evidence for deformation in the area. In this region, aplites and pegmatites are common inside and around the border of the pluton, cross-cutting different lithologies including granite, hornfels, and schist. Chemically, the aplites and pegmatites are peraluminous (Figure 2(b)) and highly fractionated, related to S-type granite (Sepahi *et al*. 2018) with high silica and alkali element contents and Light Rare Earth Elements (LREE) and High Field Strength Elements (HFSE) enrichment (Ce >103 ppm, La >125 ppm, and Nb >134 ppm), and some Large Ion Lithophile Elements

(LILEs) including Sn (>10,000 ppm), Rb (>936 ppm), and Ba (>706 ppm) (Valizadeh and Torkian 1999; Sepahi 2007; Sepahi *et al*. 2018). Sepahi *et al*. (2018) suggest that these pegmatites originated from melting of metasedimentary rocks (Figure 3), whereas Masoudi (1997) infer metamorphic to magmatic sources for some pegmatites in the Alvand complex. U-Pb dating of monzonite and zircon from aplititic and pegmatitic rocks indicates an age of 154–172 Ma (Figure 4(a)) (Sepahi *et al*. 2018), overlapping the age of the Alvand pluton. Gem deposits are found both within the Alvand granitoid and in the surrounding metamorphic complex. Deposits of garnet and beryl are found in pegmatites and metamorphic rocks (Abaru and Kamari-Zaman Abad) (Ahmadi Khalaji and Tahmasbi 2015). Deposits with coexisting tourmaline and garnet occur in pegmatites and aplites in metamorphic rocks (Mangavi) and in granitoid hosts (Ganjnameh) (Ahmadi Khalaji *et al*. 2016) (Table 1).

3.3. Boroujerd semi-gemstone district

The Boroujerd gem field near the Boroujerd granitic complex consists of ten main areas: Dehgah, Sangesefid, Ghapanvari, Gharedash, Hajiabad, Dare Seidi, Nezam abad, Astaneh, Sarsakhti and Molataleb. A significant amount of tourmaline and garnet has been produced from the Dehgah, Sangesefid, Ghapanvari, Gharedash, Hajiabad, Dare Seidi, Nezam abad, Astaneh, Sarsakhti and Molataleb sites. A significant amount of tourmaline and garnet has been produced from the Astaneh, Nezam abad, Hajiabad, Molataleb, and Sar Sakhti sites (Nekouvaght Tak and Bazargani-Guilani 2009; Khodakarami Fard *et al*. 2014; Mansouri Esfahani and Khalili 2014; Tahmasbi 2014; Rahmani Javanmard *et al*. 2018) (Table 1). These deposits are mostly metasomatic and rarely metamorphic in origin. The Boroujerd complex consists of metamorphic rocks and granitoids (Ahmadi-Khalaji *et al*. 2007; Tahmasbi *et al*. 2009; Deevsalar *et al*. 2017). Metamorphic rocks are low- to high-grade metavolcanics and metasediments (such as meta-tuffs, meta-chert, schist, and phyllite). Contact metamorphic rocks such as spotted schists, cordierite-andalusite, and cordierite-sillimanite hornfels outcrop in the northern part of the district. The Boroujerd granitic complex consists of three main units including voluminous granodiorite, small stocks of quartz diorite, and small outcrops of monzogranite in the southern Boroujerd district. These granitoids have large ranges in SiO_2 contents (52–73 wt %; Figure 2(a)). NW-trending pegmatites and aplitic dikes cross-cut the granodiorite and its metamorphic halo. Geochemically, the Boroujerd granitoid complex is metaluminous to slightly peraluminous (Figure 2(b)) I-type granite belonging to the medium to high K calc-alkaline series. The granitoids usually have low HFSE contents (Nb, Ta, and Hf) and have widely ranging Sr and Ba contents (66–484 ppm and 38–1150 ppm, respectively). They have initial $^{87}Sr/^{86}Sr$ of 0.7035–0.7110 and $\varepsilon Nd_{(t)}$ of −0.7 to −6.13 that are consistent with generation by partial melting of crustal protoliths or sediments (Ahmadi-Khalaji *et al*. 2007; Deevsalar *et al*. 2017) (Figure 4(b)). U-Pb zircon dating indicates an age range of 158–173 Ma (Figure 4(a)) for Boroujerd granitoids (Ahmadi-Khalaji *et al*. 2007; Deevsalar *et al*. 2017). Three SaSZ pegmatites have been dated: two are the same age as associated granite but pegmatite in the Ghorveh district is much younger.

Boroujerd pegmatites are LREE-enriched and their geochemical characteristics suggest that these were produced by differentiating peraluminous to slightly metaluminous (Figure 2(b)) I-type granitic magma. In contrast, Masoudi *et al*. (2009) suggest that pegmatites reflect partial melting of metasedimentary host rock. Ahmadi-Khalaji *et al*. (2007) proposed that the Boroujerd pegmatite was generated about the same time as the Boroujerd granitoid (Figure 4) in a volcanic arc to syn-collision setting (Figure 3).

4. SaSZ semi-gemstone mineralization styles

Understanding how Sanandaj–Sirjan semi-gemstone deposits formed must be first understood based on relationships with their host rocks. Tourmaline, beryl, and garnet occur in six main settings, including (1) garnet in skarns; (2) tourmaline, beryl, and garnet in pegmatite and aplitic dikes related to granodiorite and hornfels; (3) disseminations and patches of tourmaline in leucogranites; (4) quartz-tourmaline veins in granite; (5) tourmaline and garnet in metamorphic aureoles; and (6) tourmaline orbicules in aplite (Nekouvaght Tak and Bazargani-Guilani 2009; Tahmasbi *et al*. 2009; Salami *et al*. 2013, 2014; Khodakarami Fard *et al*. 2014; Mansouri Esfahani and Khalili 2014; Tahmasbi 2014; Ahmadi Khalaji and Tahmasbi 2015; Ahmadi Khalaji *et al*. 2016). These occurrences are discussed further below.

4.1. Garnet in skarn

The skarns (Figure 5(a,b)) contain carbonate (calcite), clinopyroxene (diopside) (Figure 7(a)) garnet (grossoular-andradite), vesuvianite, wollastonite, titanite and epidote.(calcite), clinopyroxene (diopside) Calcite is both primary and secondary. Clinopyroxene, wollastonite, and titanite are almost euhedral and clinopyroxene inclusions in garnet

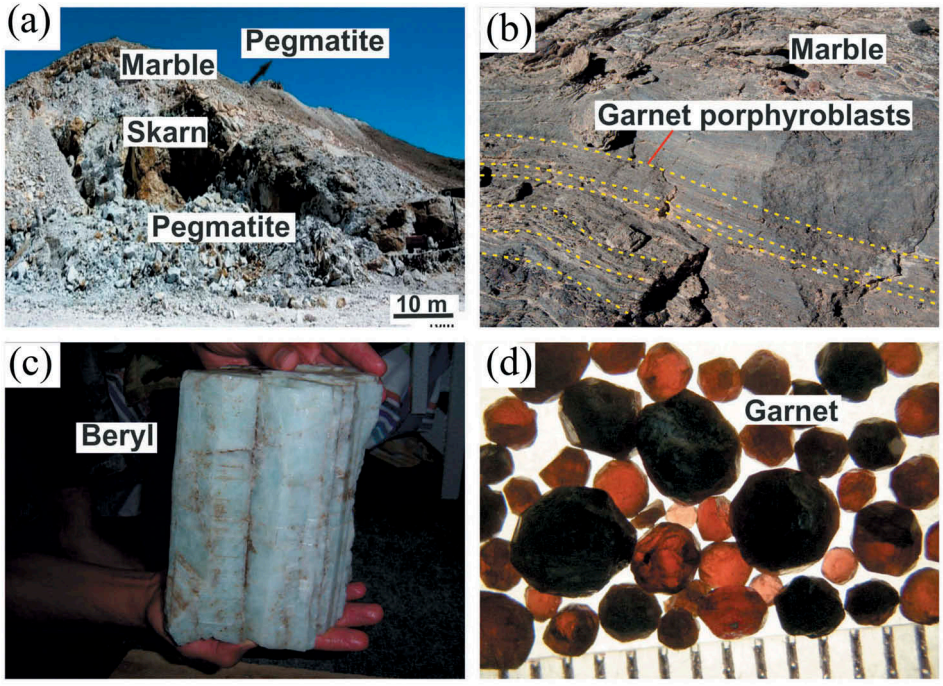

Figure 5. (a) Outcrop of Ebrahim Atar pegmatites (Ghorveh semi-gemstone district) in skarn (Mohammadi and Azizi 2017). (b) Marble with garnet porphyroclasts in Ghorveh skarn, dashed yellow lines show fine garnet porphyroclasts bands. (c) Large crystal of beryl from Ebrahim Atar pegmatite. (d) Garnets from Ebrahim Atar pegmatite.

suggests replacement of pyroxene by garnet (Figure 7(b)). Most garnets show atoll texture and have distinct resorbed margins. Garnets are partially altered and some have been pseudomorphed by chlorite, calcite, and quartz. Garnetiferous rocks are granoblastic (Sheikhi *et al*. 2012). Some skarns produce good tourmaline and garnet gems.

4.2. Tourmaline, beryl, and garnet in pegmatite and aplitic dikes

Pegmatites up to tens of centimeters thick (Figures 5(c, d) and 6(a-c)) consist of quartz, plagioclase, K-feldspar, muscovite, tourmaline, beryl and garnet. Pegmatites are equigranular, medium- to coarse-grained rocks. Pegmatites are equigranular, medium- to coarse-grained rocks. Plagioclase forms subhedral to euhedral crystals which commonly have sercitized cores where they border tourmaline. Anhedral to subhedral K-feldspars and MSs enclose small plagioclase and quartz. Quartz is anhedral, polycrystalline and shows undulose extinction. Tourmalines are columnar, up to 1 cm long, oriented perpendicular to the pegmatite margins. They are colour zoned with homogenous cores surrounded by narrow rims. Pleochroism changes from light to dark blue in the core to olive brown in narrow rims. Tourmalines are usually segmented (Figure 7(c)) by cracks filled with quartz and K-feldspar. In some cases, tourmaline is replaced by quartz. Garnets in pegmatites are sparse (Figure 7(d)) and are subhedral to euhedral with red to red brown colour and some parts contain abundant inclusions of quartz and feldspar. Fractures in the garnets are filled by quartz. Elongated beryls are widely distributed but are only abundant in the Ghorveh district where most crystals are large and fractured (Figure 7(c)). Beryl is light green, yellowish green, blue, pale yellow, or nearly white, these beryls would be classified as green beryl, aquamarine, heliodor, and goshenite varieties. Some contain MS and opaque minerals. They occur in the intermediate zone of pegmatites and typically range in size from a few millimetres to centimetres. The middles of pegmatites produce the best beryl, tourmaline, and garnet gems (Nekouvaght Tak and Bazargani-Guilani 2009; Tahmasbi *et al*. 2009; Salami *et al*. 2013, 2014; Khodakarami Fard *et al*. 2014; Tahmasbi 2014; Ahmadi Khalaji and Tahmasbi 2015; Ahmadi Khalaji *et al*. 2016).

4.3. Disseminations and patches of tourmaline in leucogranites

Host leucogranites (Figure 6(d,e)) are typically equigranular and locally porphyritic tourmalines occur as

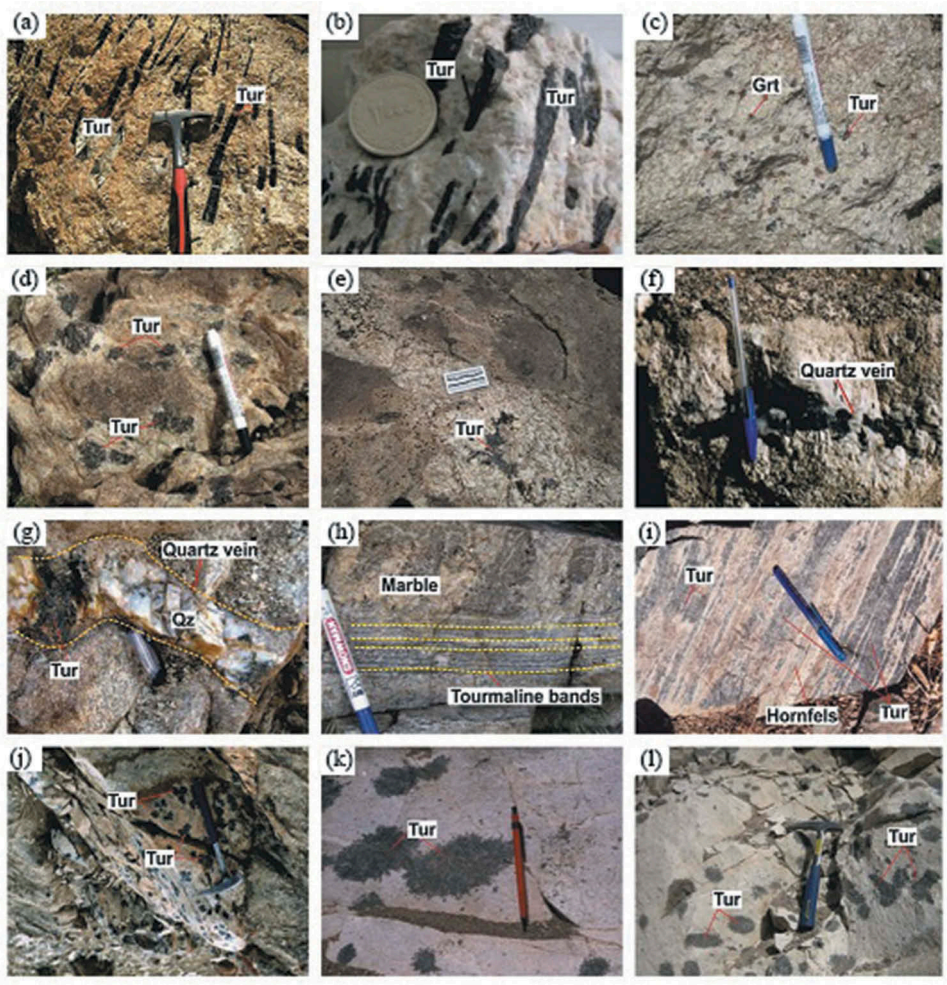

Figure 6. (a) Zaman Abad tourmalines (Tur) in pegmatites (Hamedan semi-gemstone district). (b) Zaman Abad tourmalines in pegmatites (Hamedan semi-gemstone district) (Sepahi *et al*. 2014). (c) Garnet and tourmaline in pegmatite dike from Ghaleh Samourkhan (Boroujerd semi-gemstone district). (d) Disseminations and patches of tourmaline in leucogranitic host rock from Khaku (Hamedan semi-gemstone district). (e) Patches of tourmaline in aplitic dikes (Hamedan semi-gemstone district). (f) Tourmaline-quartz vein (Hamedan semi-gemstone district). (g) Tourmaline-quartz (Qz) veins from Dehno, south of Khomein (Boroujerd semi-gemstone district) (Darvishi 2012). (h) Layers of tourmaline in metamorphic halo from Dare-Simin (Hamedan semi-gemstone district). (i) Layers of tourmaline in hornfels from Astaneh (Boroujerd semi-gemstone district) (Tahmasbi *et al*. 2009). (J) Tourmaline orbicules in granites (Hamedan semi-gemstone district). (k) Tourmaline orbicules in aplitic dikes from Dehgah (Boroujerd semi-gemstone district) (Tahmasbi 2014). (l) Tourmaline orbicules in dikes from Dehgah (Boroujerd semi-gemstone district) (Mirsepahvand *et al*. 2012).

anhedral interstitial grains (Figure 7(f)) with angular and dendritic morphologies. Tourmaline is generally unzoned. Well-developed microscopic tourmaline 'suns' are sometimes encountered in the leucogranite matrix. Quartz and K-feldspar are common around large tourmaline aggregates. K-feldspar is more abundant than plagioclase in tourmaline patches, and plagioclase with polysynthetic twins is observed locally within massive tourmalines. Some tourmaline patches produce good tourmaline gems (Nekouvaght Tak and Bazargani-Guilani 2009; Tahmasbi *et al*. 2009; Khodakarami Fard *et al*. 2014).

4.4. Quartz-tourmaline veins in granite

Quartz-tourmaline veins (Figure 6(f,g)), ranging from a few centimetres to more than 1 m thick, cross-cut the granitic rocks and are often associated with pegmatites. These veins are mostly dark (tourmaline-rich) but sometimes light coloured (quartz-rich). Vein mineralogy is simple consisting of quartz and tourmaline with medium- to fine-grained mosaic textures and small amounts of opaque minerals. In the veins, hair-like aggregates and needle crystals of tourmaline form stripes up to 2 mm thick. Typically, quartz is

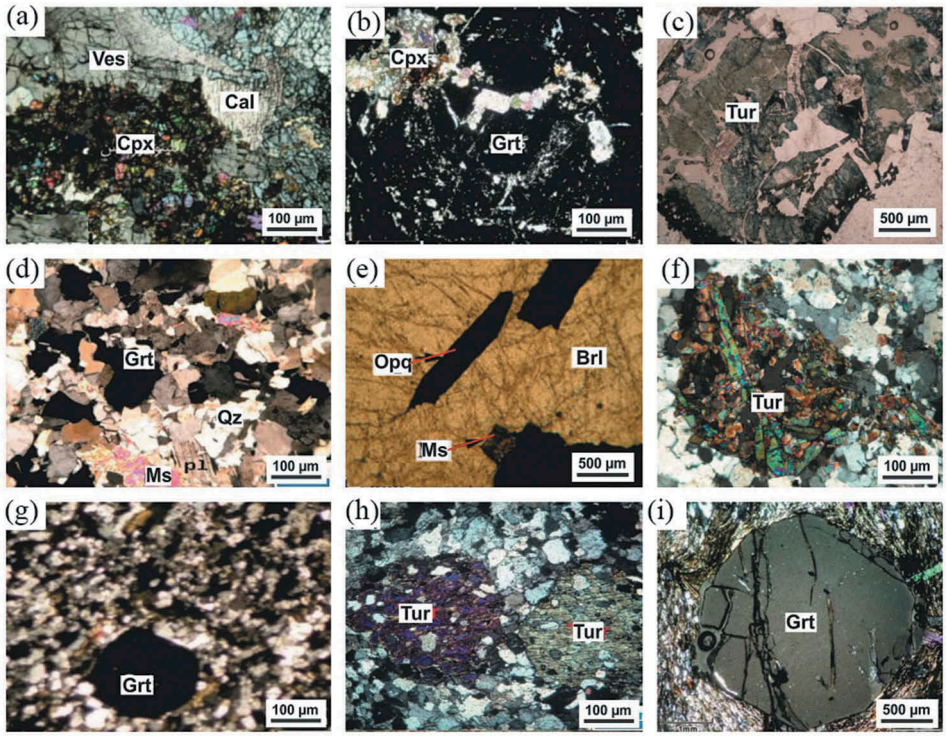

Figure 7. Photomicrographs of typical SaSZ semi-gemstones. (a) Pyroxene, vesuvianite, and calcite in skarn (Sheikhi *et al*. 2012). (b) Garnet in Ghorveh skarn (Sheikhi *et al*. 2012). (c) Tourmaline cross section in pegmatite (Tabbakh Shabani *et al*. 2013). (d) Garnet, quartz, and muscovite in aplitic rocks from Hamedan (Ahmadi Khalaji *et al*. 2016). (e) Beryl with inclusion of muscovite and opaque minerals (Salami *et al*. 2013). (F) Clusters of tourmaline in a quartz-tourmaline vein (Tabbakh Shabani *et al*. 2013). (g) Tourmaline in hydrothermal quartz vein (Nekouvaght Tak and Bazargani-Guilani 2009). (h) Tourmaline from a metapelitic schistose hornfels (Tabbakh Shabani *et al*. 2013). (I) Garnet in hornfels from Hamedan (Ahmadi Khalaji and Tahmasbi 2015). Tur: tourmaline; Grt: garnet; Brl: beryl; Qz: quartz; Ms: muscovite; Ves: vesuvianite; Cal: calcite (Whitney and Evans 2010).

milky white and shows no sign of deformation. Tourmalines may be unzoned, irregularly zoned, or have two sharply defined zones. Tourmaline with two zones forms small crystals associated with pyrite and magnetite.

4.5. Tourmaline and garnet in metamorphic aureoles

This type of tourmaline is very fine grained (<1 mm) and is associated with hornfels and metapelites (Figure 7(h)) within the contact aureole of a granitoid intrusion (Figure 6(h,i)). Tourmaline-rich zones are found along the boundary between a granitic pluton and its contact aureole. Tourmaline crystals are prismatic-acicular in shape and show strong pleochroism, with colour ranging from brown, dark green to very pale bluish-green, frequently with numerous quartz inclusions. Garnet occurs as isolated grains or clusters and euhedral grains (Figure 7(i)) that are characteristically associated with coarse- to fine-grained chlorite, andalusite, and cordierite. Tourmaline is often replaced by other minerals such as chlorite, albite, and Fe oxides (Khodakarami Fard *et al*. 2014; Ahmadi Khalaji and Tahmasbi 2015).

4.6. Tourmaline orbicules in aplites

Tourmaline orbicules (Figure 6(j-l)) are particularly well developed within aplitic dikes, which consist mainly of quartz, plagioclase, K-feldspar, biotite, and tourmaline (Tahmasbi *et al*. 2009; Tahmasbi 2014). Tourmaline orbicules typically have spherical to elliptical shapes and are 20–40 mm across.

5. Mineral chemistry

In the following sections, we summarize the mineral chemistry of semi-gemstone crystals: (1) garnet, (2) tourmaline, and (3) beryl.

5.1. Garnet chemistry

Garnets from the Ghorveh, Hamedan, and Boroujerd semi-gemstone districts have been analysed for

chemical composition (Figure 8(a)) (Sheikhi *et al*. 2012; Mansouri Esfahani and Khalili 2014; Ahmadi Khalaji and Tahmasbi 2015; Rahmani Javanmard *et al*. 2018). Garnets are generally almandine-rich, less commonly

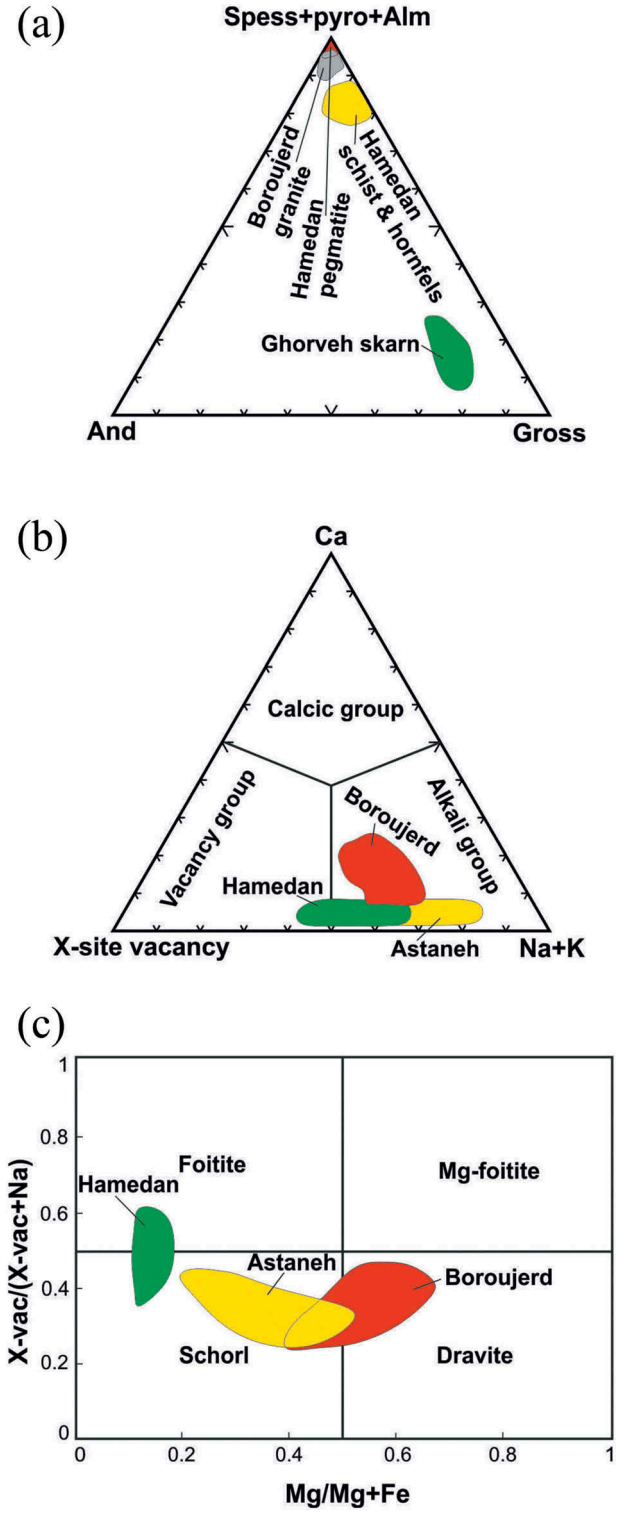

Figure 8. (a) Garnet compositions of SaSZ deposits (Einaudi et al. 1981). Data for garnets from Hamedan (Ahmadi Khalaji and Tahmasbi 2015), Molataleb (Mansouri Esfahani and Khalili 2014), Ghorveh (Sheikhi *et al*. 2012), and Boroujerd (Rahmani Javanmard *et al*. 2018). (b) Ca-K + Na-X-site vacancy ternary diagram for classifying tourmalines (Hawthorne and Henry 1999). (c) Mg/Mg + Fe *versus* X-vacancy/(X-vac + Na) for classifying tourmalines from Hamadan-Ghorveh metamorphic rocks (Hawthorne and Henry 1999; Nekouvaght Tak and Bazargani-Guilani 2009; Tahmasbi *et al*. 2009; Khodakarami Fard *et al*. 2014; Mansouri Esfahani and Khalili 2014; Tahmasbi 2014; Ahmadi Khalaji *et al*. 2016; Sepahi *et al*. 2018).

grossular- or spessartine-rich. The composition of garnet from the Ghorveh skarn is almandine 0.28, grossular 0.71, pyrope 0.00, and spessartine 0.01 (Table 1 in Sheikhi *et al*. 2012), whereas garnet from Hamedan pegmatites is almandine 0.70, grossular 0.00, pyrope 0.01, and spessartine 0.28 (Table 1 in Ahmadi Khalaji and Tahmasbi 2015). Garnets from the Boroujerd region are predominantly almandine-spessartine with lesser pyrope and grossular components ($Alm_{48.85–79.83}$, $Sps_{17.16–50.06}$, $Prp_{0.08–3.53}$, $Grs_{0.00–0.85}$) (Table 2 in Mansouri Esfahani and Khalili 2014; Table 2 in Rahmani Javanmard *et al*. 2018). Pegmatitic garnets from Hamedan and Boroujerd are homogenous, with almandine slightly increasing while spessartine decreases from core to rim. Schist-hosted garnets in the Hamedan metamorphic halo contain less almandine (0.63) and pyrope (0.07) component than do garnets with hornfels host (almandine 0.80 and pyrope 0.13) (Table 1 in Ahmadi Khalaji and Tahmasbi 2015). Despite the modest effect of temperature on garnet morphology, temperature gradients may control crystal morphologies so that most garnet crystals with varying CaO and MnO in hornfels and aplites are trapezohedrons rather than dodecahedrons. Dodecahedrons may be produced under low-temperature gradients in schists, but trapezohedrons are produced with high-temperature gradients (Sepahi 2007).

Thermobarometric studies of SaSZ metamorphic rocks show that garnet schists formed at 4.3 ± 0.5 kbar (14 km deep in the crust) and 568–586° C, whereas garnet hornfelses formed at 2.5 ± 0.1 kbar (9 km) and 539–569°C (Baharifar 1997). In contrast, Ghorveh garnets formed at <3 kbar (<10 km) and 450–587°C (Sheikhi *et al*. 2012) (Table 1).

5.2. Tourmaline chemistry

Five types of tourmaline have been distinguished based on field geology and mineral assemblages (Nekouvaght Tak and Bazargani-Guilani 2009; Tahmasbi *et al*. 2009; Gholami and Mokhtari Khodakarami Fard *et al*. 2014; Mansouri Esfahani and Khalili 2014; Tahmasbi 2014; Ahmadi Khalaji *et al*. 2016): (1) tourmaline in pegmatite and aplitic dikes related to granodiorite and hornfels; (2) disseminations and patches of tourmaline in leucogranites; (3) quartz-tourmaline veins in granite; (4) tourmaline in metamorphic aureoles; and (5) tourmaline orbicules in aplite.

In terms of tourmaline classification (Hawthorne and Henry 1999), most are alkali type with minor X-site vacancies and Ca substituting for Na (Figure 8(b)). They are mostly schorl and dravite, with minor foitite (Figure 8(c)) (Nekouvaght Tak and Bazargani-Guilani 2009; Tahmasbi *et al*. 2009; Khodakarami Fard *et al*. 2014; Mansouri Esfahani and Khalili 2014; Tahmasbi 2014; Ahmadi Khalaji *et al*. 2016). Nearly all samples of SaSZ tourmaline do not have enough Si to fill the tetrahedral sites. The six octahedral Z sites are occupied by Al but the three octahedral Y sites contain a variety of divalent cations. In fact, the main compositional variable of tourmaline is the occupancy of Y site. The sum of T + Z + Y cations in the tourmaline ideal formula is 15. The X-site ranges from 0.63 to 1.12 and the X-site vacancy is smallest in hornfels and schist tourmaline and the largest in pegmatite tourmaline. Na is dominant over Ca and K in X-sites in all samples. Ca contents are low, ranging from 0.0 to 0.24 apfu. B_2O_3 ranges from 9.90 to 12.92 wt%. Fe^{2+} content varies a lot (0.80–1.96 apfu.), whereas Al varies less, between 5.83 and 7.02 apfu (Table 1 in Ahmadi Khalaji *et al*. 2016). In all samples, FeO contents are greater than MgO. Pegmatite tourmaline has the highest Fe/Mg value (Table 1 in Ahmadi Khalaji *et al*. 2016), whereas tourmalines from leucogranite, country rocks, quartz veins, and metamorphic haloes show the lowest Fe/Mg value (Nekouvaght Tak and Bazargani-Guilani 2009; Tahmasbi *et al*. 2009; Khodakarami Fard *et al*. 2014; Mansouri Esfahani and Khalili 2014; Tahmasbi 2014). Pegmatite tourmalines have higher concentrations of Fe and lower concentrations of Mg (Nekouvaght Tak and Bazargani-Guilani 2009; Ahmadi Khalaji *et al*. 2016) than those in the granite, quartz veins, and country rock.

Major and trace element abundances of tourmalines were controlled by their pegmatite host. Pegmatitic tourmalines that do not coexist with garnet have elevated contents of Ga, Zn, Sn, and Zr; large ion lithophile elements like Sr; and REEs relative to those associated with garnet (Ahmadi Khalaji *et al*. 2016). This conclusion is in agreement with statement that tourmaline chemistry mostly reflects the compositional nature of its host melt and or fluid (Van Hinsberg *et al*. 2011).

5.3. Beryl chemistry

Analysed beryls show a slight excess of Si. This is attributed to high silica activity in the crystallizing melt, which is assigned to the Be tetrahedron. Beryls in Ebrahim Atar pegmatite have very low contents of MnO, TiO_2, CaO, and K_2O (Table 1 in Salami *et al*. 2013); the low amount of alkali element minerals indicates direct crystallization from magma because hydrothermal beryl contains more alkali elements (Markl and Schumacher 1997; Wang *et al*. 2009; Salami *et al*. 2013). Beryls in Ebrahim Atar pegmatite contain 108–123 ppm Cs and 9–12 ppm V. Elevated Cs contents can be explained by enrichment of this

element in the pegmatitic siliceous and hydrous fluid (Salami *et al*. 2013).

Evensen *et al*. (1999) demonstrated that the solubility of Be is strongly affected by differing fluid concentrations of SiO_2, Al_2O_3 (i.e. beryl saturation), and F (Wood 1992). They explained that F-related complexes can carry a lot of Be in aqueous fluids (Barton and Young 2002). Wood (1992) showed how low Ca contents in fluids are essential for Be movement, because elevated Ca contents will crystallize fluorite, so preventing the complexing of Be with F. Silica and alumina activities are also important because low SiO_2 activity in the fluid favours precipitation of chrysoberyl, phenakite, and bromellite (Barton and Young 2002). Very high Al_2O_3 fluids favour precipitation of chrysoberyl or euclase, whereas very low Al_2O_3 contents favour formation of phenakite or bertrandite (Barton and Young 2002). Thus, the peraluminous nature of the Ghorveh pegmatite (Azizi *et al*. 2016) may have favoured precipitation of Be-alumosilicates such as chrysoberyl and euclase.

6. Boron and oxygen isotopic constraints

The two main isotopic constraints for SaSZ semi-gemstone genesis come from B and O isotopes. B isotopes are especially useful for understanding the origin of tourmaline, because this mineral contains so much B, typically ~10 wt% B_2O_3 (Foit *et al*. 1989). Figure 9(a) summarizes what we know about the $\delta^{11}B$ isotopic composition of SaSZ semi-gemstone deposits, based on 41 analyses (Esmaeily *et al*. 2009). The $\delta^{11}B$ values of tourmaline in hydrothermal quartz veins range from −2.3‰ to −11.7‰ (Esmaeily *et al*. 2009), broadly similar to many igneous rocks and typical continental crust (Nekouvaght Tak and Bazargani-Guilani 2009). The mantle range in B isotopes is from −4‰ to −10‰ (Dixon *et al*. 2017). Sediments and crust vary between +5‰ and −5‰ depending on lithology and degree of seawater alteration (Ishikawa and Nakamura 1993; Smith *et al*. 1995). This overlap is consistent with the hypothesis that semi-gemstone-mineralizing fluids were largely sweated out of SaSZ metasediments.

The $\delta^{18}O$ values of five quartz samples from hydrothermal quartz-tourmaline veins are in the range of +11.9‰ to +13.8‰ (average 13.4%) (Figure 9(b)) (Nekouvaght Tak and Bazargani-Guilani 2009). These O isotopic compositions are similar to metamorphic or magmatic-metamorphic waters (Rollinson 1993; Hoefs 2004), indicating that semi-gemstone-mineralizing fluids formed through dehydration of hydrous minerals during metamorphism (Hoefs 2004).

7. Discussion

Here, we explore two related topics concerning the Sanandaj–Sirjan semi-gemstone province: (1) types of SaSZ pegmatites and (2) geological conditions of gem mineralization.

7.1. Types of SaSZ pegmatites

Whole rock analyses of pegmatites from the Ghorveh, Hamedan, and Boroujerd regions show that these contain ~75 wt% SiO_2 and ~16 wt% Al_2O_3 as well as highly variable Na_2O (1.58–7.64 wt%) and K_2O (0.70–6.68 wt%). These compositions indicate a very evolved magma, perhaps reflecting the final expulsion of hot fluid- and silica-rich melt(s) from the solidifying granite. Pegmatites show peraluminous to slightly metaluminous natures, and based on Alumina Saturation Index (ASI) these types of pegmatites are commonly related to orogenic S- and I-type granitic magmas (Sepahi 1999; 2008; Azizi *et al*. 2016; Ahmadi-Khalaji *et al*. 2007; Rahmani Javanmard *et al*. 2018; Sepahi *et al*. 2018).

Pegmatites are classified based on their depth of emplacement and relationship to metamorphism and associated granitic plutons. Ginsburg *et al*. (1979) identified five classes (abyssal, MS, muscovite-rare element (MSREL), rare-element, and miarolitic) (Figure 10). Abyssal pegmatites form in granulite facies metamorphic terranes (lower crust, >15 km deep) and display no direct relationship with granitic bodies. Miarolitic pegmatites form 1.5–3.5 km deep (Černý 1982; ČErný and Ercit 2005) and are the shallowest of the pegmatites (Černý 1982; ČErný and Ercit 2005). REE pegmatites crystallize 3.5–7 km deep. These are interpreted to be fractionation products of differentiated granites (Černý 1982; ČErný and Ercit 2005). Mica-bearing pegmatites crystallize 7–11 km deep and are hosted by amphibolite-facies metamorphic rocks (Černý 1982; ČErný and Ercit 2005). These mica-rich, rare-element poor magmas represent direct products of sediment anatexis or are magmas separated from anatectic, autochthonous granites (Černý 1982).

SaSZ pegmatites fall in the MS and MSREL classes (Salami *et al*. 2014; Azizi *et al*. 2016; Rahmani Javanmard *et al*. 2018; Sepahi *et al*. 2018), although they formed a bit shallower than most MS pegmatites. Figure 10 shows that SaSZ pegmatites formed at 3.5–7.5 kbar and 550–650°C, corresponding to 10–25 km deep in the crust, suggesting an elevated temperature gradient of 22–65°C/km.

Černý (1991) and ČErný and Ercit (2005) split pegmatites into two compositional types: NYF and LCT types. The acronyms NYF and LCT stand for the trace elements that are most enriched in the fractionation sequences of

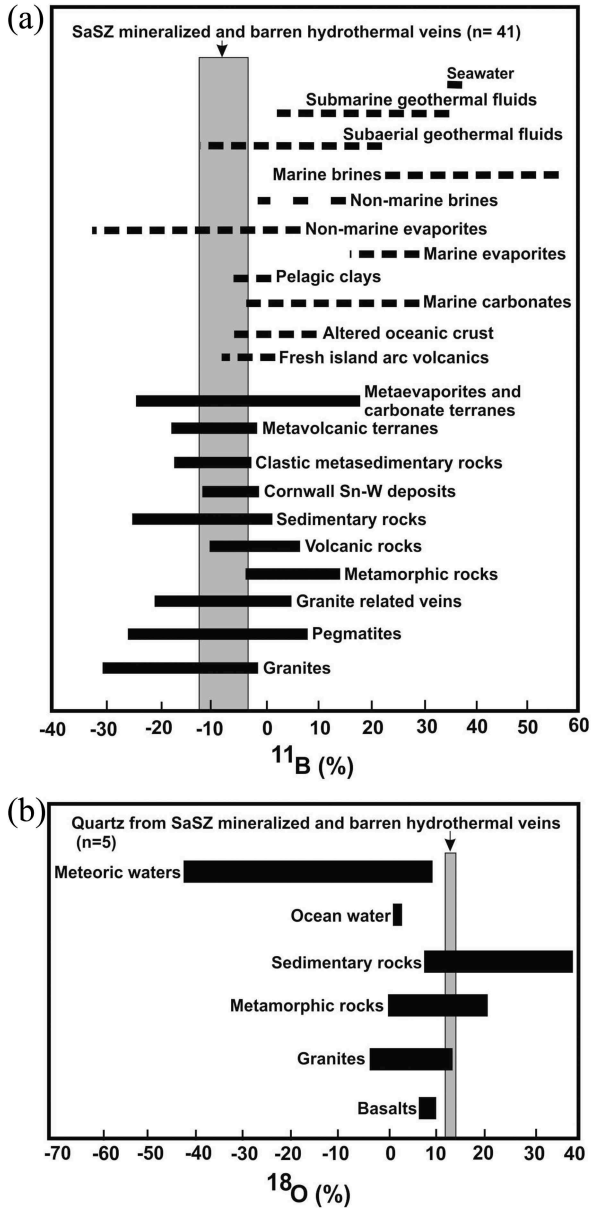

Figure 9. Isotopic data for Sanandaj–Sirjan semi-gemstone deposits. (a) Boron isotopes. The variation of B isotope values in tourmaline from various environments (solid lines) compared with B isotopic compositions of significant B reservoirs (dashed lines). Data are from Byerly and Palmer (1991), range variation from Hoefs (2004). Data for Boroujerd (Nezam abad) B isotopes from Esmaeily *et al*. (2009). (b) Oxygen isotopes, range variation from Hoefs (2004). Data for Boroujerd (Nezam abad) O isotopes from Nekouvaght Tak and Bazargani-Guilani (2009).

these two families (Nb, Y, and REE, F *versus* Li, Cs, and Ta, also B, P, and F). Salami *et al*. (2014), Azizi *et al*. (2016), and Sepahi *et al*. (2018) report LCT affinity for pegmatites from the Ghorveh and Hamedan semi-gemstone districts. LCT pegmatites are peraluminous (London 1996) but are mostly associated with metaluminous granites. LCT pegmatite magma can also be generated from supracrustal metasediments and as well as lower crystal granulites

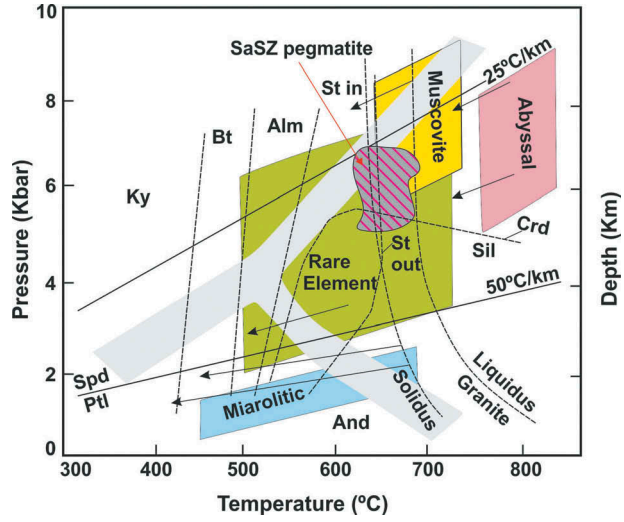

Figure 10. Pressure and temperature relationships of SaSZ semi-gemstone deposits compared with the four major categories of pegmatites. MSC: Muscovite; AB: Abyssal; RE: Rare Element; MI: Miarolitic (after Ginsburg 1984; Černý 1991). Arrows indicate evolutionary trends relative to metamorphic grades of host rocks. Mineral assemblages indicate that SaSZ gem minerals were generated at 3.5–7.5 kbar and 550–650°C, corresponding to 11.5–25 km deep in the continental crust. Sil: sillimanite; Ky: kyanite; And: andalusite; Alm: almandine; Bt: biotite; St: staurolite; Crd: cordierite; Spd: spodumene; Ptl: petalite (Whitney and Evans 2010).

(Černý 1991; London 1996; ČErný and Ercit 2005). LCT pegmatites are related to subduction and post-tectonic extension in continental collision belts (Martin and De Vito 2005; Tkachev 2011).

7.2. Geological conditions of gem mineral formation

Below we discuss how SaSZ gem minerals formed. First, we discuss tourmaline, then beryl, then garnet.

7.2.1 Tourmaline

Tourmaline is the earliest mineral produced from a dense silica-rich aqueous melt as it cools, assuming there is enough B, Al, Mg, and Fe for making tourmaline. Clay minerals and organic materials are potential sources for boron (Henry and Guidotti 1985; Henry and Dutrow 1990) and thus psammopelitic metasediments contain sufficient B, Al, Mg, Fe, Ca, and Na to produce tourmaline through reaction of boron-rich fluids with feldspars, phyllosilicates, and other minerals (Morgan and London 1989; Fuchs and Lagache 1994; London *et al*. 1996). Boron in SaSZ metamorphic rocks probably was concentrated in clay minerals with adsorbed boron (Henry and Dutrow 1996). During prograde metamorphism, B may have been released from the clays

in the pelitic protolith. Rising temperatures around a cooling pluton results in dehydration metamorphic reactions which will also mobilize boron. Released boron can mix with magmatic fluids to form tourmaline. Tourmaline compositions in SaSZ metamorphic rocks show affinities with metapelites and metapsammites (Figure 11) (Nekouvaght Tak and Bazargani-Guilani 2009; Tahmasbi *et al*. 2009; Khodakarami Fard *et al*. 2014; Mansouri Esfahani and Khalili 2014; Tahmasbi 2014).

As a result, the granitoid and metamorphic hosts are widely distributed and cut by many dikes that are S- and rarely I-type pegmatites and aplites (Nekouvaght Tak and Bazargani-Guilani 2009; Tahmasbi *et al*. 2009; Khodakarami Fard *et al*. 2014; Mansouri Esfahani and Khalili 2014; Tahmasbi 2014; Ahmadi Khalaji *et al*. 2016; Rahmani Javanmard *et al*. 2018; Sepahi *et al*. 2018) (Figure 12). SaSZ pegmatites generally reflect magmatic fluids expelled during advanced fractional crystallization of granitic magmas (London *et al*. 2001; Burianek *et al*. 2011). With progressive melt fractionation pegmatites are progressively enriched in Rb, Cs, Be, Sn, Ta, Nb and often also in B, P, and F (Salami *et al*. 2013; Azizi *et al*. 2016; Rahmani Javanmard *et al*. 2018; Sepahi *et al*. 2018). Inger and Harris (1993) emphasized that contents of Ba, Ca, and K in anatectic melts are strongly influenced by the presence of water during partial melting (Conrad *et al*. 1988; Holtz and Johannes 1991; Patino Douce and Harris 1998; Kawakami 2001; Burianek *et al*. 2011; Müller *et al*. 2012; Weinberg and Hasalová 2015). As granite melts cool and become more viscous (Baker and Vaillancourt 1995), boron-bearing dense hydrous fluids may separate from residual magma due to its much lower viscosity. Thus, the presence of trace amounts of boron contained in aluminosilicate minerals in the parent peraluminous magma source may be sufficient to produce tourmaline in pegmatite and aplites via aluminosilicate breakdown during low degrees of partial melting (Nabelek *et al*. 1992). This is confirmed by tourmaline compositions in SaSZ pegmatite and aplite rocks that show affinities with granitoids and their associated pegmatites and aplites (Figure 11) (Nekouvaght Tak and Bazargani-Guilani 2009; Tahmasbi *et al*. 2009; Khodakarami Fard *et al*. 2014; Mansouri Esfahani and Khalili 2014; Tahmasbi 2014). This contrasts with tourmaline compositions in SaSZ metamorphic rocks, as discussed above.

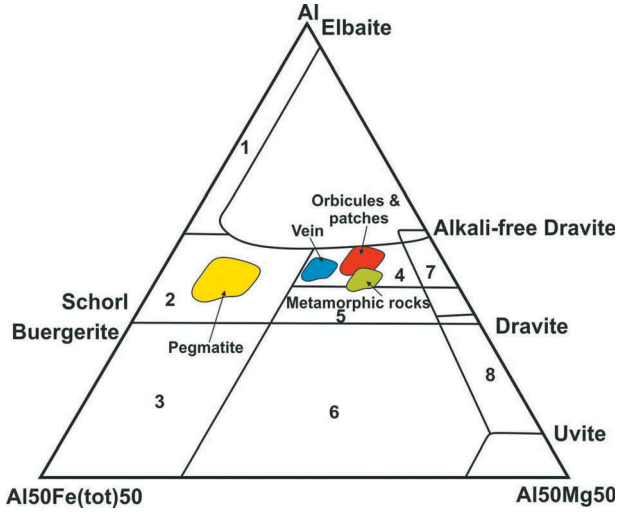

Figure 11. Average composition of studied tourmalines plotted in triangular Al-Fetot-Mg diagram (Henry and Guidotti 1985). Fields: 1 – Li-rich granitoids, pegmatites, and aplites; 2 – Granitoids and associated pegmatites and aplites; 3 – Hydrothermally altered granites; 4 – Metapelites and metapsammites coexisting with an Al-saturated phase; 5 – Metapelites and metapsammites not coexisting with Al-saturated phase; 6 – Fe^{3+}-rich quartz-tourmaline rocks, calc silicate rocks, and metapelites; 7 – Metaultramafics with low Ca; 8 – Meta carbonates and metapyroxenites.

Tourmaline nodules and orbicules in the SaSZ aplites formed from post-magmatic metasomatism by boron-rich hydrothermal fluids derived from the crystallization of granite magma along cracks (Figure 11) (Rozendaal and Bruwer 1995; Burianek and Novak 2003; Hezel *et al*. 2011; Tabbakh Shabani *et al*. 2013; Tahmasbi 2014; Hong *et al*. 2017). Tourmaline patches and orbicules are commonly dispersed below the roof zones of aplites as scattered masses or clusters (Burianek *et al*. 2011; Tahmasbi 2014; Hong *et al*. 2017) resulting from devolatilization and phase separation of hydrous boron-rich fluid from granitic melts (Samson and Sinclair 1992; Sinclair and Richardson 1992; Jiang *et al*. 2003; Shewfelt 2005; Dini *et al*. 2007; Trumbull *et al*. 2008; Balen and Broska 2011). In this situation, boron will be concentrated in silicic melts, but will ultimately segregate into a bubble-rich aqueous phase (Dingwell *et al*. 1996; London *et al*. 1996; Veksler and Thomas 2002; Veksler 2004). Depending on lithostatic pressure, vapour bubbles can separate from a melt at a low degree of crystallization, and rise up between grains as bubble-laden plumes or tubules (Burianek and Novak 2003; Hezel *et al*. 2011; Tabbakh Shabani *et al*. 2013; Tahmasbi 2014; Hong *et al*. 2017). Increasing pressure around the pluton due to volatile degassing, together with crystallization of tourmaline and other minerals, will enlarge the deformed zone and open spaces for boron-rich fluids to occupy. As crystallization continues and magmatic viscosity increases, small bubbles may join to produce tubules channelling flow to the top of the intrusion. When the supply of vapour is reduced, bubble-laden plumes solidify, ultimately creating irregular tourmaline-rich patches among coarse-grained igneous crystals (Hong *et al*. 2017). Irregular

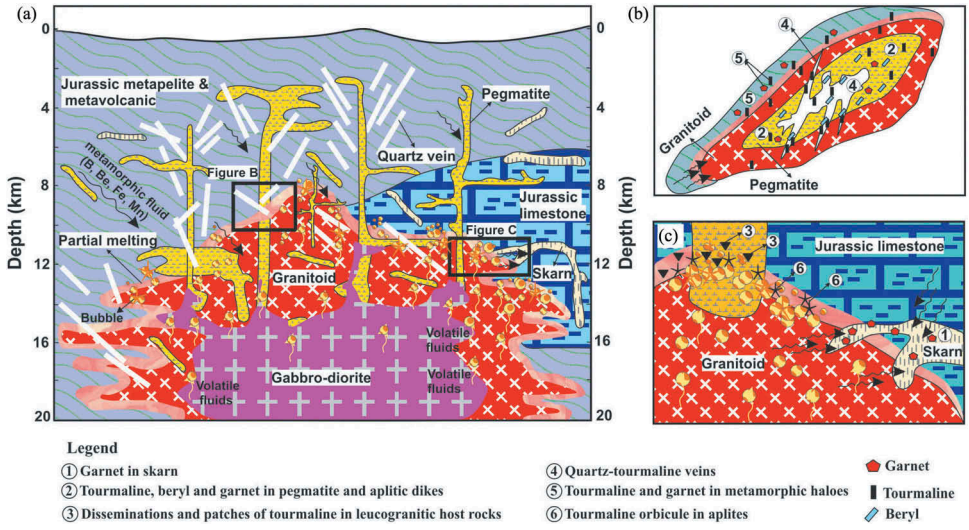

Figure 12. (a) Sketch illustrating the formation of skarn, quartz vein, and pegmatite in the SaSZ tourmaline–garnet ± beryl semi-gemstone province. The injection of mafic magma in Jurassic time increased the temperature in the continental crust and metasediments, ultimately producing granitic melts and related pegmatite (garnet, tourmaline, and beryl), skarn (garnet), and quartz veins (tourmaline). (b) Sketch of mineralization of tourmaline, beryl, and garnet in granite, pegmatite, vein, and metamorphic halo. The pegmatite dikes in the granitoid and metamorphic halo may have been produced by expulsion and crystallization of hydrous melts of metapelites in the contact aureole of SaSZ granitoid complexes. In the final step of pegmatite melt evolution, the removal of aqueous fluids formed quartz veins with tourmaline. Tourmaline nodules and orbicules in the granitic rocks formed from post-magmatic metasomatic alteration related to boron-rich hydrothermal fluids derived from the crystallization of highly evolved granitic melts along cracks. (c) Sketch of garnet mineralization in skarn. During metamorphism, decarbonization and dehydration reactions released large amounts of CO_2 and H_2O which migrated towards fractures. Fracture formation and mineralization is a main aspect for forming garnet by providing channels for flow of magmatic volatiles and products obtained from thermal metamorphic reactions as skarn.

tourmaline patches disseminated in aplites are understood to reflect small boron-rich volatile bubbles, while the spherical tourmaline orbicules and cavities solidified in the uppermost portions of granite plutons are likely to be relicts of large trapped bubbles of exsolved magmatic fluid (Tahmasbi *et al*. 2009; Tahmasbi 2014; Hong *et al*. 2017).

Increasing lithostatic pressure and tectonic activity often leads to fracture of the surrounding wall rocks. Boron-rich aqueous fluids invade these fractures, hydrothermally altering the host rocks, and finally healing the fractures by mineral precipitation. Field relations indicate that quartz-tourmaline veins were the final stage of SaSZ magmatic fluid evolution (Figure 12) (Nekouvaght Tak and Bazargani-Guilani 2009; Tahmasbi *et al*. 2009; Khodakarami Fard *et al*. 2014). Field evidence together with geochemical and petrographic data shows that only a minor fraction of the melt was saturated in tourmaline (Nekouvaght Tak and Bazargani-Guilani 2009; Sheikhi *et al*. 2012; Khodakarami Fard *et al*. 2014). The presence of graphite in SaSZ granitoids is further evidence for metasediment assimilation (Radfar 1987; Ahmadi-Khalaji *et al*. 2007; Nekouvaght Tak and Bazargani-Guilani 2009). This allowed evolved B-rich fluids to infiltrate along lithological boundaries and shear zones around the pluton. On the other hand, the $\delta^{11}B$ values of tourmaline-quartz veins in the Nezam abad deposit (Boroujerd semi-gemstone district; Figure 9(a)) look like those of the metamorphosed pyroclastic-sedimentary and metavolcanic terranes (Esmaeily *et al*. 2009). This is confirmed by tourmaline composition of quartz veins that show some affinities with metapelites and metapsammites (Figure 11) (Nekouvaght Tak and Bazargani-Guilani 2009; Tahmasbi *et al*. 2009; Khodakarami Fard *et al*. 2014; Mansouri Esfahani and Khalili 2014; Tahmasbi 2014).

7.2.2 Beryl

Beryl is found in Ebrahim Atar (Ghorveh) and Zaman Abad (Hamedan) pegmatites. Crystal fractionation of pegmatitic melts enriches the residual magmatic fluid in incompatible elements such as Be. It is not clear what was the source of Be for forming beryl in pegmatites. Because Be has a very small ionic radius (0.27 Å) and low charge (+2), it prefers tetrahedral coordination (Hawthone and Huminicki 2002). Minerals such as cordierite, plagioclase, and phyllosilicates in SaSZ metamorphic rocks can contain significant non-essential Be in their mineral structures (ČErný 2002; Franz and Morteani 2002). Plagioclase and MS can have high Be concentrations (~200 and ~150 ppm respectively)

(Evensen *et al*. 1999; Grew 2002; London and Evensen 2002). Cordierite can contain up to ~8100 ppm Be (Evensen and London 2002) and staurolite contains up to ~150 ppm Be (Grew *et al*. 2001; Grew 2002). Breakdown of these minerals may be the source of Be to produce pegmatitic beryls.

Barton and Young (2002) subdivided Be mineralization based on ASI, silica saturation, and alkalinity, including (1) strongly to weakly peraluminous, (2) metaluminous and weakly peraluminous, and (3) peralkaline. Of these, peraluminous magmas are most favourable for beryl mineralization, due to their favourable SiO_2 and Al_2O_3 contents. The most favourable intrusions for forming beryl are ultrafractionated, moderately peraluminous S- and I-type granitoid magmas with low Ca and high F concentrations, which can yield fertile epigenetic hydrothermal fluids that favour beryl precipitation. Very high Al_2O_3 fluid activities favour precipitation of chrysoberyl or euclase, whereas very low Al_2O_3 fluid activities favour formation of phenakite or bertrandite. So, the main source of Be for generating beryl in Ebrahim Atar and Zaman Abad pegmatites may have been derived from breakdown of phyllosilicate minerals and feldspars associated with a strongly peraluminous granitic magma (Azizi *et al*. 2016). As Figure 2(b) shows, the Ebrahim Atar and Hamedan pegmatite is strongly peraluminous.

7.2.3 Garnet

SaSZ garnets are limited to pegmatites, aplites, adjacent metamorphic rocks, and other metamorphic rocks far from contact. Pegmatite and aplite garnets are all members of the almandine-spessartine solid-solution series, with igneous compositions (Miller and Stoddard 1981). They have high spessartine (17–50 mol%) and almandine (49–80 mol%) contents, whereas pyrope and andradite components are minor. The absence of reaction rims, euhedral shapes, and spessartine >50 mol% indicates that the garnets in pegmatite and aplite crystallized at low pressure from these melts. It is suggested that an exsolved aqueous phase from the melt complexed accessible Mn and mixed with SaSZ pegmatite melts to form spessartine. Müller *et al*. (2012) showed that a range in MnO/(FeO + MnO) ratio of garnets reveals progressive magmatic differentiation.

The disappearance of biotite during the last stages of fractional crystallization favours formation of garnetiferous aplites and pegmatites (Abbot 1981). In extremely fractionated granitic magmas such as pegmatites (Bogoch *et al*. 1997), the very low abundances of Fe result in very minor little or no biotite crystallizing. In the absence of biotite, the stability of spessartine garnet increases, which may partly be reflected in Mn enrichment in rims. If and when MS crystallizes, the melt moves to the liquid-garnet-MS cotectic and Fe/Mg and Mn/Fe content of the melt rises (Miller and Stoddard 1981). It is proposed that segregation of an aqueous phase from the granitic melt transported Mn and Fe to the peripheries (Figure 12), allowing garnet crystallization below 700°C (Clarke 1981; Manning 1983; Burianek *et al*. 2011; Moore *et al*. 2015). As a result, the MnO/(FeO + MnO) content of garnet rises with increasing melt fractionation, which is partly controlled by the presence or absence of coexisting Mn- and Fe-bearing minerals (Müller *et al*. 2012). In this case, the MnO/(FeO + MnO) of garnet can be used to indicate the degree of fractionation of the melt from which it formed. Garnets from less fractionated pegmatites are typically Fe rich (Müller *et al*. 2012). Garnets from aplites and pegmatites are often Fe-Mn rich, and exhibit obvious core to rim decrease in Mn (Baldwin and von Knorring 1983; Whitworth 1992; Gadas *et al*. 2013), whereas garnets from granitoids are mostly Fe rich and show weak core-to-rim increase in Mn (Day *et al*. 1992; Harangi *et al*. 2001; Koepke *et al*. 2003; Samadi *et al*. 2014). The wide variations noted above in almandine and spessartine components indicate low to moderate degrees of pegmatite evolution, suggesting that high Mn content in garnet reflects more fractionated magmas. It is therefore possible that crystallization of spessartine-rich garnets in SaSZ pegmatites reflects enrichment of the magma in volatile constituents at low pressures and temperatures. At the final steps of pegmatite development, the removal of aqueous fluids formed quartz veins and skarns rich in tourmaline and garnet (Figure 12) (Nekouvaght Tak and Bazargani-Guilani 2009; Sheikhi *et al*. 2012; Khodakarami Fard *et al*. 2014).

The formation of SaSZ skarns (Sheikhi *et al*. 2012) can be ascribed to the contact metamorphic effects of intrusions into limestones associated with shearing along minor faults. During metamorphism, decarbonation and dehydration reactions yield significant CO_2 and H_2O which can mix with magmatic fluids and flow into faults and fractures; these processes are important for garnet mineralization in skarn.

8. Conclusions

We have six main conclusions from our study:

(1) The SaSZ semi-gemstone province is identified and subdivided into three districts: Ghorveh, Hamedan, and Boroujerd. The SaSZ semi-gemstone province is characterized by the abundance of tourmaline and garnet, sometimes also beryl.
(2) Tourmalines are concentrated in a variety of lithologies related to Jurassic intrusions: metamorphic rocks, quartz veins, patches, orbicules, pegmatites,

and granitic rocks, reflecting pervasive mobilization and concentration of B around these intrusions.

(3) SaSZ pegmatites fall in the MS and MSREL classes and formed at 3.5–7.5 kbar and 550–650°C, corresponding to 10–25 km deep in the crust, suggesting an elevated regional temperature gradient of 22–65°C/km. The geochemical and mineralogical characteristics of the pegmatites reveal high contents of silica and alkali elements, indicating extreme fractionation.

(4) Tourmalines belong to schorl-dravite solid solution, with compositions largely controlled by the composition of the wall-rock hosts. Metapelites provided the essential Fe, Mg, and Al contents for forming tourmaline, but B may be derived from granitic magma as well as metasediments. Magmatic fractionation, metamorphism, and anatexis created tourmaline-bearing pegmatite dikes along the contact between granites and metamorphic rocks. Quartz-tourmaline veins are explained as products of crystallization of fluids exsolved from the granitic melt and surrounding metasediments. In contrast, magmatic-hydrothermal volatile exsolution and fluxing of boron-rich aqueous fluids exsolved from the crystallizing granitic magma during emplacement into shallow crust was responsible for forming tourmaline patches, orbicules, and cavities.

(5) Garnets in pegmatites have igneous compositions and belong to the almandine-spessartine solid-solution series. It is suggested that exsolution of one or more aqueous phases from the granitic melt locally evolved Mn and Fe concentrations locally to allow garnet crystallization. In contrast, fractures in limestone formed by regional deformation provided channels for flow of magmatic volatiles and produced garnet, pyroxene, and wollastonite from thermal metamorphic reactions as skarn.

(6) Further research is needed to test and refine these ideas and better understand tourmaline–garnet ± beryl mineralization of the SaSZ semi-gemstone province.

Acknowledgements

We thank A.A. Baharifar, A. Ahmadi Khalaji, Z. Tahmasbi, M. Mansouri Esfahani, M.A. Nekouvaght Tak, Z. Gholami, A.A Tabakh Shabani, A.A. Sepahi, S. Salami, N. Daneshvar, M. Komailian N. Shabanian, A.R. Davoudian, F. Sheikhi, and B. Rahmizadeh for sharing photos and chemical data used in this paper. The UTD Geosciences contribution number is 1336.

Disclosure statement

No potential conflict of interest was reported by the authors.

Funding

This work was supported by the This is UTD Geosciences contribution number 13xx [13xx];

ORCID

Hossein Azizi http://orcid.org/0000-0001-5686-4340

References

Abbott, R.N., Jr., 1981, AFM liquidus projections for granitic magmas, with special reference to hornblende, biotite and garnet: Canadian Mineralogist, 19, 103–110.

Ahmadi Khalaji, A., and Tahmasbi, Z., 2015, Mineral chemistry of garnet in pegmatite and metamorphic rocks in the Hamedan area: Journal of Economic Geology, 7, 243–258. ISSN 2008-7306 *(in Persian)*.

Ahmadi Khalaji, A., Tahmasbi, Z., Zal, F., and Shabani, Z., 2016, The behavior of major and trace elements of the tourmaline from the Mangavai and Ganjnameh pegmatitic rocks (Hamadan area): Iranian Journal of Petrology, 27, 1–24. doi:10.22108/ijp.2016.21015.

Ahmadi-Khalaji, A.A., Esmaeily, D., Valizadeh, M.V., and Rahimpour-Bonab, H., 2007, Petrology and geochemistry of the granitoid complex of boroujerd, sanandaj-sirjan zone, western Iran: Journal of Asian Earth Sciences, 29, 859–877. doi:10.1016/j.jseaes.2006.06.005.

Alavi, M., 1994, Tectonics of the Zagros orogenic belt of Iran: New data and interpretations: Tectonophysics, 229, 211–238. doi:10.1016/0040-1951(94)90030-2.

Aliani, F., Maanijou, M., Sabouri, Z., and Sepahi, A.A., 2012, Petrology, geochemistry and geotectonic environment of the alvand intrusive complex, Hamedan, Iran: Chemie der Erde-Geochemistry, 72, 363–383. doi:10.1016/j.chemer.2012.05.001.

Alipour, S., Abedini, A., and Talaie, B., 2015, Geochemical characteristics of the Qahr-Abad fluorite deposit, southeast of Saqqez, western Iran: Arabian Journal of Geosciences, 8, 7309–7320. *(in Persian)* doi:10.1007/s12517-014-1747-6.

Arvin, M., Pan, Y., Dargahi, S., Malekizadeh, A., and Babaei, A., 2007, Petrochemistry of the Siah-Kuh granitoid stock southwest of Kerman, Iran: Implications for initiation of Neotethys subduction: Journal of Asian Earth Sciences, 30, 474–489. doi:10.1016/j.jseaes.2007.01.001.

Azizi, H., and Asahara, Y., 2013, Juvenile granite in the Sanandaj–Sirjan Zone, NW Iran: Late Jurassic–Early Cretaceous arc–Continent collision: International Geology Review, 55, 1523–1540. doi:10.1080/00206814.2013.782959.

Azizi, H., Asahara, Y., Mehrabi, B., and Chung, S.L., 2011, Geochronological and geochemical constraints on the petrogenesis of high-K granite from the Suffi abad area, Sanandaj-Sirjan Zone, NW Iran: Chemie der Erde-Geochemistry, 71, 363–376. doi:10.1016/j.chemer.2011.06.005.

Azizi, H., Beiranvand, M.Z., and Asahara, Y., 2015b, Zircon U–Pb ages and petrogenesis of a tonalite–Trondhjemite–Granodiorite (TTG) complex in the Northern Sanandaj–

Sirjan Zone, Northwest Iran: Evidence for Late Jurassic arc–Continent collision: Lithos, 216–217, 178–195. doi:10.1016/j.lithos.2014.11.012.

Azizi, H., Mohammadi, K., Asahara, Y., Tsuboi, M., Daneshvar, N., and Mehrabi, B., 2016, Strongly peraluminous leucogranite (Ebrahim-Attar granite) as evidence for extensional tectonic regime in the Cretaceous, Sanandaj Sirjan zone, northwest Iran: Chemie der Erde-Geochemistry, 76, 529–541. doi:10.1016/j.chemer.2016.08.006.

Azizi, H., and Moinevaziri, H., 2009, Review of the tectonic setting of Cretaceous to Quaternary volcanism in northwestern Iran: Journal of Geodynamics, 47, 167–179. doi:10.1016/j.jog.2008.12.002.

Azizi, H., Najari, M., Asahara, Y., Catlos, E.J., Shimizu, M., and Yamamoto, K., 2015a, U–Pb zircon ages and geochemistry of Kangareh and Taghiabad mafic bodies in northern Sanandaj–Sirjan Zone, Iran: Evidence for intra-oceanic arc and back-arc tectonic regime in Late Jurassic: Tectonophysics, 660, 47–64. doi:10.1016/j.tecto.2015.08.008.

Baharifar, A., Moinevaziri, H., Bellon, H., and Piqué, A., 2004, The crystalline complexes of Hamadan (Sanandaj–Sirjan zone, western Iran): Metasedimentary Mesozoic sequences affected by Late Cretaceous tectono-metamorphic and plutonic events: Comptes Rendus Geoscience, 336, 1443–1452. doi:10.1016/j.crte.2004.09.014.

Baharifar, A.A., 1997, New perspective on petrogenesis of the regional metamorphic rocks of Hamedan area, Iran [M.Sc thesis]: Tarbiat Moallem University of Tehran. *(in persian)*.

Baker, D.R., and Vaillancourt, J., 1995, The low viscosities of F and H_2O bearing granitic melts and implications for melt extraction and transport: Earth and Planetary Science Letters, 132, 199–211. doi:10.1016/0012-821X(95)00054-G.

Baldwin, J.R., and von Knorring, O., 1983, Compositional range of Mn-garnet in zoned granitic pegmatites: The Canadian Mineralogist, 21, 683–688.

Balen, D., and Broska, I., 2011, Tourmaline nodules: Products of devolatilization within the final evolutionary stage of granitic melt: Geological Society, London, Special Publications 350, 53–68. doi:10.1144/SP350.4.

Barton, M.D., and Young, S., 2002, Non-pegmatitic deposits of beryllium: Mineralogy, geology, phase equilibria and origin: Reviews in Mineralogy and Geochemistry, 50, 591–691. doi:10.2138/rmg.2002.50.14.

Bayati, M., Esmaeily, D., Maghdour-Mashhour, R., Li, X.H., and Stern, R.J., 2017, Geochemistry and petrogenesis of kolahghazi granitoids of iran: iInsights into the jurassic sanandaj-sirjan magmatic arc: Chemie Der Erde-gGeochemistry, v. 77, p. 281-302. doi: 10.1016/j.chemer.2017.02.003.

Berberian, F., and Berberian, M., 1981, Tectono-plutonic episodes in Iran: Zagros Hindu Kush Himalaya Geodynamic Evolution, edited by Gupta, H.K., and Delany, F.M., American Geophysical Union, Vol. 3, 33–69.

Berberian, F., Muir, I.D., Pankhurst, R.J., and Berberian, M., 1982, Late Cretaceous and early Miocene Andean-type plutonic activity in northern Makran and Central Iran: Journal of the Geological Society, 139, 605–614. doi:10.1144/gsjgs.139.5.0605.

Bernard, S., Horsfield, B., Schulz, H.M., Wirth, R., Schreiber, A., and Sherwood, N., 2012, Geochemical evolution of organic-rich shales with increasing maturity: A STXM and TEM study of the Posidonia Shale (Lower Toarcian, northern Germany): Marine and Petroleum Geology, 31, 70–89. doi:10.1016/j.marpetgeo.2011.05.010.

Bogoch, R., Bourne, J., Shirav, M., and Harnois, L., 1997, Petrochemistry of a Late Precambrian garnetiferous granite, pegmatite and aplite, southern Israel: Mineralogical Magazine, 61, 111–122. doi:10.1180/minmag.1997.061.404.11.

Bordenave, M.L., and Hegre, J.A., 2005, The influence of tectonics on the entrapment of oil in the Dezful Embayment, Zagros Fold belt, Iran: Journal of Petroleum Geology, 28, 339–368. doi:10.1111/j.1747-5457.2005.tb00087.

Burianek, D., Hanzl, P., and Hrdlickova, K., 2011, Pegmatite dykes and quartz veins with tourmaline: An example of partial melting in the contact aureole of the Chandman Massif intrusion, SW Mongolia: Journal of Geosciences, 56, 201–213. doi:10.3190/jgeosci.091.

Burianek, D., and Novak, M., 2003, Tourmaline orbicules in leucogranites as indicator of geochemical fractionation of late solidus to early subsolidus magmatic fluids: Journal of Geosciences, 48, 0–30.

Byerly, G.R., and Palmer, M.R., 1991, Tourmaline mineralization in the Barberton greenstone belt, South Africa: Early Archean metasomatism by evaporite-derived boron: Contributions to Mineralogy and Petrology, 107, 387–402. doi:10.1007/BF00325106.

Černý, P., 1982, Anatomy and classification of granitic pegmatites, Cerny, P. ed. Granitic pegmatites in science and industry: mineralogical association of Canada, Short Course Handbook, Vol. 8, 1–39.

Černý, P., 1991, Rare-element granitic pegmatites. Part I: Anatomy and internal evolution of pegmatitic deposits: Geoscience Canada, 18, 49-67.

Černý, P., 2002, Mineralogy of beryllium in granitic pegmatites: Reviews in Mineralogy and Geochemistry, 50, 405–444. doi:10.2138/rmg.2002.50.10.

Černý, P., and Ercit, T.S., 2005, The classification of granitic pegmatites revisited: The Canadian Mineralogist, 43, 2005–2026. doi:10.2113/gscanmin.43.6.2005.

Chiu, H.Y., Chung, S.L., Zarrinkoub, M.H., Mohammadi, S.S., Khatib, M.M., and Iizuka, Y., 2013, Zircon U–Pb age constraints from Iran on the magmatic evolution related to Neotethyan subduction and Zagros orogeny: Lithos, 162, 70–87. doi:10.1016/j.lithos.2013.01.006.

Clark, B., Blauwet, D., Schmitz, F., Stephan, T., Müller, S., Laurs, B.M., Mayerson, W.M., Williams, C., Williams, B., Link, K., and Boehm, E., 2016, Gem Notes: The Journal of Gemology, 35, 96. doi:10.15506/JoG.2016.35.2.96.

Clarke, D.B., 1981, The mineralogy of peraluminous granites; a review: The Canadian Mineralogist, 19, 3–17.

Conrad, W., Nicholls, I., and Wall, V.J., 1988, Water saturated, and undersaturated melting of metaluminous, and peraluminous crustal compositions at 10 kb: Evidence for the origin of silicic magmas in the Taupo volcanic zone, New Zealand, and other occurrences: Journal of Petrology, 29, 765–803. doi:10.1093/petrology/29.4.765.

Cox, K.G., Bell, J.D., and Pankhurst, R.J., 1979, The interpretation of igneous rocks, George Allen and Unwin.

Darvishi, E., 2012, Petrography and geochemistry of Dehno granite: Journal of Environmental Geology, 19, 17–30.

Davoudian, A.R., Genser, J., Dachs, E., and Shabanian, N., 2008, Petrology of eclogites from north of Shahrekord, Sanandaj-

Sirjan Zone, Iran: Mineralogy and Petrology, 92, 393–413. doi:10.1007/s00710-007-0204-6.

Day, R.A., Green, T.H., and Smith, I.E.M., 1992, The origin and significance of garnet phenocrysts and garnet-bearing xenoliths in Miocene calc-alkaline volcanics from Northland, New Zealand: Journal of Petrology, 33, 125–161. doi:10.1093/petrology/33.1.125.

Deevsalar, R., Shinjo, R., Liégeois, J.P., Valizadeh, M.V., Ahmadian, J., Yeganehfar, H., Murata, M., and Neill, I., 2017, Subduction-related mafic to felsic magmatism in the Malayer–Boroujerd plutonic complex, western Iran: Swiss Journal of Geosciences, 1–25. doi:10.1007/s00015-017-0287-y.

Dingwell, D.B., Hess, K.U., and Knoche, R., 1996, Granite and granitic pegmatite melts: Volumes and viscosities: Earth and Environmental Science Transactions of the Royal Society of Edinburgh, 87, 65–72. doi:10.1017/S0263593300006489.

Dini, A., Corretti, A., Innocenti, F., Rocchi, S., and Westerman, D.S., 2007, Sooty sweat stains or tourmaline spots? The Argonauts on the Island of Elba (Tuscany) and the spread of Greek trading in the Mediterranean Sea, Geological Society: London, Special Publications, Vol. 273, 227–243. doi:10.1144/GSL.SP.2007.273.01.18

Dixon, J.E., Bindeman, I.N., Kingsley, R.H., Simons, K.K., Le Roux, P. J., Hajewski, T.R., Swart, P., Langmuir, C.H., Ryan, J.G., Walowski, K.J., Wada, I., and Wallace, P.J., 2017, Light stable isotopic compositions of enriched mantle sources: Resolving the Dehydration Paradox: Geochemistry, Geophysics, Geosystems, 8, 3801–3839. doi:10.1002/2016GC006743.

Eftekharnejad, J., 1981, Tectonic division of Iran with respect to sedimentary basins: Journal of Iranian Petroleum Society, 82, 19–28. *(in Persian)*.

Einaudi, M.T., Meinert, L.D., and Newberry, R.J., 1981, Skarn deposits: Economic Geology, 75th Anniversary, v. 317–391.

Esmaeily, D., Nédélec, A., Valizadeh, M.V., Moore, F., and Cotten, J., 2005, Petrology of the Jurassic Shah-Kuh granite (eastern Iran), with reference to tin mineralization: Journal of Asian Earth Sciences, 25, 961–980. doi:10.1016/j.jseaes.2004.09.003.

Esmaeily, D., Trumbull, R.B., Haghnazar, M., Krienitz, M.-S., and Wiedenbeck, M., 2009, Chemical and boron isotopic composition of hydrothermal tourmaline from scheelite-quartz veins at Nezam abad, western Iran: European Journal of Mineralogy, 21, 347–360. doi:10.1127/0935-1221/2009/0021-1908.

Esna-Ashari, A., Tiepolo, M., Valizadeh, M.V., Hassanzadeh, J., and Sepahi, A.A., 2012, Geochemistry and zircon U–Pb geochronology of Aligoodarz granitoid complex, Sanandaj-Sirjan zone, Iran: Journal of Asian Earth Sciences, 43, 11–22. doi:10.1016/j.jseaes.2011.09.001.

Evensen, J.M., and London, D., 2002, Experimental silicate mineral/melt partition coefficients for beryllium and the crustal Be cycle from migmatite to pegmatite: Geochimica et Cosmochimica Acta, 66, 2239–2265. doi:10.1016/S0016-7037(02)00889-X.

Evensen, J.M., London, D., and Wendlandt, R.F., 1999, Solubility and stability of beryl in granitic melts: American Mineralogist, 84, 733–745. doi:10.2138/am-1999-5-606.

Foit, F.F., Fuchs, Y., and Myers, P.E., 1989, Chemistry of alkali-deficient schorls from two tourmaline-dumortierite deposits: American Mineralogists, 74, 1317–1324.

Franz, G., and Morteani, G., 2002, Be-minerals: Synthesis, stability, and occurrence in metamorphic rocks: Reviews in Mineralogy and Geochemistry, 50, 551–589. doi:10.2138/rmg.2002.50.13.

Fuchs, Y., and Lagache, M., 1994, La transformation chlorite-tourmaline en milieu hydrothermal, exemples naturels et approche experimentale: Comptes Rendus de l'Académie des Sciences: Série 2 Sciences de la Terre et des Planètes, 319, 907–913.

Gadas, P., Novák, M., Talla, D., and Galiová, M.V., 2013, Compositional evolution of grossular garnet from leucotonalitic pegmatite at Ruda nad Moravou, Czech Republic; a complex EMPA, LA-ICP-MS, IR and CL study: Mineralogy and Petrology, 107, 311–326. doi:10.1007/s00710-012-0232-8.

Ghasemi, A., and Talbot, C.J., 2006, A new tectonic scenario for the Sanandaj–Sirjan Zone (Iran): Journal of Asian Earth Sciences, 26, 683–693. doi:10.1016/j.jseaes.2005.01.003.

Ghorbani, M., 2003, Precious stones and minerals (Semi-gemstones) and their position in Iran, Pars Geology Research Center, 396.

Ginsburg, A.I., 1984, The geological condition of the location and the formation of granitic pegmatites, In Proceedings of the 27th International Geological Congress, v. 15, p. 245–260.

Ginsburg, A.I., Timofeyev, I.N., and Feldman, L.G., 1979, Principles of geology in the granitic pegmatites: Nedra, Moscow, 296. *(In Russian)*.

Golonka, J., 2004, Plate tectonic evolution of the southern margin of Eurasian the Mesozoic and Cenozoic: Tectonophysics, 381, 235–273. doi:10.1016/j.tecto.2002.06.004.

Grew, E.S., 2002, Mineralogy, petrology and geochemistry of beryllium: An introduction and list of beryllium minerals: Reviews in Mineralogy and Geochemistry, 50, 1–76. doi:10.2138/rmg.2202.50.01.

Grew, E.S., Hålenius, U., Kritikos, M., and Shearer, C.K., 2001, New data on welshite, eg Ca2Mg3. 8Mn2+ 0.6 Fe2+ 0.1 Sb5 + 1.5O2 [Si2. 8Be1. 7Fe3+ 0.65 Al0. 7As0.17O18], an aenigmatite-group mineral: Mineralogical Magazine, 65, 665–674. doi:10.1180/002646101317018488.

Groat, L.A., Giuliani, G., Marshall, D.D., and Turner, D., 2008, Emerald deposits and occurrences: A review: Ore Geology Reviews, 34, 87–112. doi:10.1016/j.oregeorev.2007.09.003.

Groat, L.A., and Laurs, B.M., 2009, Gem formation, production, and exploration: Why gem deposits are rare and what is being done to find them: Elements, v. 5, p. 153–158. doi:10.2113/gselements.5.3.153.

Groat, L.A., Turner, D.J., and Evans, R.J., 2014, 13.23: Gem deposits: Reference Module in Earth Systems and Environmental Sciences, 13, 592–622. doi:10.1016/B978-0-08-095975-7.01126-8.

Harangi, S.Z., Downes, H., Kósa, L., Szabó, C.S., Thirlwall, M.F., Mason, P.R.D., and Mattey, D., 2001, Almandine garnet in calc-alkaline volcanic rocks of the Northern Pannonian Basin (Eastern–Central Europe): Geochemistry, petrogenesis and geodynamic implications: Journal of Petrology, 42, 1813–1843. doi:10.1093/petrology/42.10.1813.

Hassanzadeh, J., Stockli, D.F., Horton, B.K., Axen, G.J., Stockli, L.D., Grove, M., Schmitt, A.K., and Walker, J.D., 2008, U-Pb zircon geochronology of late Neoproterozoic–Early Cambrian granitoids in Iran: Implications for paleogeography, magmatism and exhumation history of Iranian basement: Tectonophysics, 451, 71–96. doi:10.1016/j.tecto.2007.11.062.

Hawthorne, F.C., and Henry, D.J., 1999, Classification of the minerals of the tourmaline group: European Journal of Mineralogy, 11, 201–215. doi:10.1127/ejm/11/2/0201.

Henry, D.J., and Dutrow, B.L., 1990, Ca substitution in Li-poor aluminous tourmaline: The Canadian Mineralogist, 28, 111–124.

Henry, D.J., and Dutrow, B.L., 1996, Metamorphic tourmaline and its petrologic applications: Reviews in Mineralogy and Geochemistry, 33, 503-557.

Henry, D.J., and Guidotti, C.V., 1985, Tourmaline as a petrogenetic indicator mineral- An example from the staurolite-grade metapelites of NW Maine: American Mineralogist, 70, 1–15. 0003-004x/85/0I 0 2-000l $02.00.

Hezel, D.C., Kalt, A., Marschall, H.R., Ludwig, T., and Meyer, H.P., 2011, Major-element and Li, Be compositional evolution of tourmaline in an S-type granite–Pegmatite system and its country rocks: An example from Ikaria, Aegean Sea, Greece: The Canadian Mineralogist, 49, 321–340. doi:10.3749/canmin.49.1.321.

Hoefs, J., 2004, Stable Isotope Geochemistry, Springer-Verlag, Berlin, 150 p.

Holtz, F., and Johannes, W., 1991, Genesis of peraluminous granites I. Experimental investigation of melt composition at 3 and 5 kb and various H_2O activities: Journal of Petrology, 32, 935–958. doi:10.1093/petrology/32.5.935.

Honarmand, M., Li, X.H., Nabatian, G., and Neubauer, F., 2017, In-situ zircon U-Pb age and Hf-O isotopic constraints on the origin of the Hasan-Robat A-type granite from Sanandaj–Sirjan zone, Iran: Implications for reworking of Cadomian arc igneous rocks: Mineralogy and Petrology, 111, 659–675. doi:10.1007/s00710-016-0490-y.

Hong, W., Cooke, D.R., Zhang, L., Fox, N., and Thompson, J., 2017, Tourmaline-rich features in the Heemskirk and Pieman Heads granites from western Tasmania, Australia: Characteristics, origins, and implications for tin mineralization: American Mineralogist, 102, 876–899. doi:10.2138/am-2017-5838.

Hosseiny, M., 1999, Geological map of Ghorveh: Geology survey of Iran, Scale 1/100000. No. 5560.

Huong, L.T.T., Häger, T., Hofmeister, W., Hauzenberger, C., Schwarz, D., Van Long, P., Wehmeister, U., Khoi, N.N., and Nhung, N.T., 2012, Semi-gemstones from Vietnam: An Update: Gems and Gemology, 48. doi:10.5741/GEMS.48.3.158.

Inger, S., and Harris, N., 1993, Geochemical constraints on leucogranite magmatism in the Langtang Valley, Nepal Himalaya: Journal of Petrology, 34, 345–368. doi:10.1093/petrology/34.2.345.

Ishikawa, T., and Nakamura, E., 1993, Boron isotope systematics of marine sediments. Earth and Planetary Science Letters, v.117, p. 567–580. doi: 10.1016/0012-821X(93)90103-G.

Jiang, S.Y., Yang, J.H., Novák, M., and Selway, J., 2003, Chemical and boron isotopic compositions of tourmaline from the Lavicky leucogranite, Czech Republic: Geochemical Journal, 37, 545–556. doi:10.2343/geochemj.37.545.

Kawakami, T., 2001, Boron depletion controlled by the breakdown of tourmaline in the migmatite zone of the Aoyama area, Ryoke metamorphic belt, southwestern Japan: The Canadian Mineralogist, 39, 1529–1546. doi:10.2113/gscanmin.39.6.1529.

Kazmin, V.G., Sbortshikov, I.M., Ricou, L.E., Zonenshain, L.P., Boulin, J., and Knipper, A.L., 1986, Volcanic belts as markers of the Mesozoic-Cenozoic active margin of Eurasia: Tectonophysics, 123, 123–152. doi:10.1016/0040-1951(86)90195-2.

Khodakarami Fard, Z., Zarei Sahameih, R., and Khodakarami Fard, A., 2014, Composition of tourmaline in leucogranite, Pegmatite, quartz veins and their country rocks from Hajiabad area, Boroujerd, NW Iran: Journal of Novel Applied Sciences, 3-6, 661–672.

Kievlenko, E., 2003, Geology of Gems, Soregaroli, A. ed., Ocean Pictures Ltd, Littleton, CO, 432.

Koepke, J., Falkenberg, G., Rickers, K., and Diedrich, O., 2003, Trace element diffusion and element partitioning between garnet and andesite melt using synchrotron X-ray fluorescence microanalysis (μ-SRXRF): European Journal of Mineralogy, 15, 883–892. doi:10.1127/0935-1221/2003/0015-0883.

London, D., 1996, Granitic pegmatites: Earth and Environmental Science Transactions of the Royal Society of Edinburgh, 87, 305–319. doi:10.1017/S0263593300006702.

London, D., and Evensen, J.M., 2002, Beryllium in silicic magmas and the origin of beryl-bearing pegmatites: Reviews in Mineralogy and Geochemistry, 50, 445–486. doi:10.2138/rmg.2002.50.11.

London, D., Evensen, J.M., Fritz, E., Icenhower, J.P., Morgan, G. B., and Wolf, M.B., 2001, Enrichment and accommodation of manganese in granite-pegmatite systems: In Eleventh Annual VM Goldschmidt Conference. Abstract #3369. LPI Contribution, No. 1088, Lunar and Planetary Institute, Houston (CD-ROM).

London, D., Morgan, G.B.V.I., and Wolf, M.B., 1996, Boron in granitic rocks and their contact aureoles: Reviews in Mineralogy and Geochemistry, 33, 299–330.

Maanijou, M., Aliani, F., and Miri, M., 2011, Geochemistry and petrology of granophyric granite veins penetrated in the igneous intrusive complex in south of Ghorveh Area, west Iran: Australian Journal of Basic and Applied Sciences, 5, 926–934. ISSN 1991-8178.

Mahmoudi, S., Corfu, F., Masoudi, F., Mehrabi, B., and Mohajjel, M., 2011, U–Pb dating and emplacement history of granitoid plutons in the northern Sanandaj–Sirjan Zone, Iran: Journal of Asian Earth Sciences, 41, 238–249. doi:10.1016/j.jseaes.2011.03.006.

Malek-Mahmoudi, F., Davoudian, A.R., Shabanian, N., Azizi, H., Asahara, Y., Neubauer, F., and Dong, Y., 2017, Geochemistry of metabasites from the North Shahrekord metamorphic complex, Sanandaj-Sirjan Zone: Geodynamic implications for the Pan-African basement in Iran: Precambrian Research, 293, 56–72. doi:10.1016/j.precamres.2017.03.003.

Maniar, P.D., and Piccoli, P.M., 1989, Tectonic discrimination of granitoids: Geological Society of America Bulletin, 101, 635–643. doi:10.1130/0016-7606(1989)101%3C0635:TDOG%3E2.3.CO;2.

Manning, D.A.C., 1983, Chemical variation in garnets from aplites and pegmatites, peninsular Thailand: Mineralogical Magazine, 47, 353–358. doi:10.1180/minmag.1983.047.344.10.

Mansouri Esfahani, M., and Khalili, M., 2014, Mineralogy and mineral – Chemistry of tourmaline and garnet from Molataleb village granitoid (North of Aligudarz) NW of Isfahan: Iranian Journal of Crystallography and Mineralogy, 22, 139–148. ijcm.ir/article-1-259-fa.html. *(in Persian)* .

Markl, G., and Schumacher, J.C., 1997, Beryl stability in local hydrothermal and chemical environments in a mineralized granite: American Mineralogist, 82, 194–202. doi:10.2138/am-1997-1-221.

Martin, R.F., and De Vito, C., 2005, The patterns of enrichment in felsic pegmatites ultimately depend on tectonic setting:

The Canadian Mineralogist, 43, 2027–2048. doi:10.2113/gscanmin.43.6.2027.

Masoudi, F., 1997, Contact metamorphism and pegmatites development in the region SW of Arak, Iran. [Ph.D. thesis]: University of Leeds, UK, 321 p.

Masoudi, F., Mehrabi, B., Rezai Aghdam, M., and Yardley, B.W. D., 2009, The nature of fluids during pegmatite development in metamorphic terrains: Evidence from Hamadan complex, Sanandaj-Sirjan metamorphic zone, Iran: Journal of the Geological Society of India, 73, 407–418. doi:10.1007/s12594-009-0020-1.

Mazhari, S.A., Bea, F., Amini, S., Ghalamghash, J., Molina, J.F., Montero, P., Scarrow, J.H., and Williams, I.S., 2009, The Eocene bimodal Piranshahr massif of the Sanandaj–Sirjan Zone, NW Iran: A marker of the end of the collision in the Zagros orogeny: Journal of the Geological Society, 166, 53–69. doi:10.1144/0016-76492008-022.

Meen, V.B., and Tushigham, A.D., 1968, Crown Jewels of Iran, University of Toronto Press, Toronto, 159.

Miller, C.F., and Stoddard, E.F., 1981, The role of manganese in the paragenesis of magmatic garnet: An example from the Old Woman-Piute Range, California: The Journal of Geology, 89, 233–246. doi:10.1086/628582.

Mirsepahvand, F., Tahmasbi, Z., Shahrokhi, S.V., Ahmadi Khalaji, A., and Khalili, M., 2012, Geochemistry and source determination of tourmalines in Boroujerd area, Vol. 20, 281–292. doi:ijcm.ir/article-1-380-en.html.

Moghadam, H.S., Khademi, M., Hu, Z., Stern, R.J., Santos, J.F., and Wu, Y., 2015, Cadomian (Ediacaran–Cambrian) arc magmatism in the Chah Jam–Biarjmand metamorphic complex (Iran): Magmatism along the northern active margin of Gondwana: Gondwana Research, 27, 439–452. doi:10.1016/j.gr.2013.10.014.

Moghadam, H.S., Li, X.H., Stern, R.J., Santos, J.F., Ghorbani, G., and Pourmohsen, M., 2016, Age and nature of 560–520 Ma calc-alkaline granitoids of Biarjmand, northeast Iran: Insights into Cadomian arc magmatism in northern Gondwana: International Geology Review, 58, 1492–1509. doi:10.1080/00206814.2016.1166461.

Mohajjel, M., and Fergusson, C.L., 2000, Dextral transpression in Late Cretaceous continental collision, Sanandaj–Sirjan zone, western Iran: Journal of Structural Geology, 22, 1125–1139. doi:10.1016/S0191-8141(00)00023-7.

Mohajjel, M., and Fergusson, C.L., 2014, Jurassic to Cenozoic tectonics of the Zagros Orogen in northwestern Iran: International Geology Review, 56, 263–287. doi:10.1080/00206814.2013.853919.

Mohajjel, M., Fergusson, C.L., and Sahandi, M.R., 2003, Cretaceous–Tertiary convergence and continental collision, Sanandaj–Sirjan zone, western Iran: Journal of Asian Earth Sciences, 21, 397–412. doi:10.1016/S1367-9120(02)00035-4.

Mohajjel, M., and Izadikian, L., 2007, Poly-deformed Tectonites in Dome Structure of the Almabolagh Region, West of Hamadan: Geosciences, Geological Survey of Iran, 66, 116–133.

Mohammadi, K., and Azizi, H., 2017, The role of tetrad effects in distribution of rare earth elements in Ebrahim-Attar granitoid body, Southwest Ghorveh, with emphasis on the geochemical twins: Kharazmi Journal of Earth Sciences, 2, 247–270. gnf.khu.ac.ir/article-1-2566-fa.html. *(in Persian)* .

Moore, S.J., Cesare, B., and Carlson, W.D., 2015, Epitaxial nucleation of garnet on biotite in the polymetamorphic metapelites surrounding the Vedrette di Ries intrusion (Italian Eastern Alps): European Journal of Mineralogy, 27, 5–18. doi:10.1127/ejm/2015/0027-2414.

Morgan, G.B., and London, D., 1989, Experimental reactions of amphibolite with boron-bearing aqueous fluids at 200 MPa: Implications for tourmaline stability and partial melting in mafic rocks: Contributions to Mineralogy and Petrology, 102, 281–297. doi:10.1007/BF00373721.

Müller, A., Kearsley, A., Spratt, J., and Seltmann, R., 2012, Petrogenetic implications of magmatic garnet in granitic pegmatites from southern Norway: The Canadian Mineralogist, 50, 1095–1115. doi:10.3749/canmin.50.4.1095.

Nabelek, P.I., Russ-Nabelek, C., and Haeussler, G.T., 1992, Stable isotope evidence for the petrogenesis and fluid evolution in the Proterozoic Harney Peak leucogranite, Black Hills, South Dakota: Geochimica et Cosmochimica Acta, 56, 403–417. doi:10.1016/0016-7037(92)90141-5.

Nadimi, A., and Konon, A., 2012, Strike-slip faulting in the central part of the Sanandaj-Sirjan Zone, Zagros Orogen, Iran: Journal of Structural Geology, 40, 2–16. doi:10.1016/j.jsg.2012.04.007.

Nekouvaght Tak, M.A., and Bazargani-Guilani, K., 2009, Chemical Variation of Tourmaline and Source of Hydrothermal Solutions in Nezam Abad W-(Sn) Ore Deposit, Sanandaj-Sirjan Zone, West-Central Iran: Journal of Sciences, Islamic Republic of Iran, 20, 115–126. ISSN 1016-1104

Patino Douce, A.E., and Harris, N., 1998, Experimental constraints on Himalayan anatexis: Journal of Petrology, 39, 689–710. doi:10.1093/petroj/39.4.689.

Pearce, J.A., Harris, N.B., and Tindle, A.G., 1984, Trace element discrimination diagrams for the tectonic interpretation of granitic rocks: Journal of Petrology, 25, 956–983. doi:10.1093/petrology/25.4.956.

Radfar, J., 1987, Petrology of granitic rocks from Astaneh area, Iran [MSc thesis]: University of Tehran, 111 p.

Rahmani Javanmard, S., Tahmasbi, Z., Ding, X., Khalaji, A.A., and Hetherington, C.J., 2018, Geochemistry of garnet in pegmatites from the Boroujerd Intrusive Complex, Sanandaj-Sirjan Zone, western Iran: Implications for the origin of pegmatite melts: Mineralogy and Petrology, 1–20. doi:10.1007/s00710-018-0591-x.

Rollinson, H., 1993, Using geochemical data: Evaluation, presentation, interpretation, Langman Group UK Limited, 352.

Rozendaal, A., and Bruwer, L., 1995, Tourmaline nodules: Indicators of hydrothermal alteration and Sn Zn (W) mineralization in the Cape Granite Suite, South Africa: Journal of African Earth Sciences, 21, 141–155. doi:10.1016/0899-5362(95)00088-B.

Salami, S., Sepahi, A.A., and Maanijou, M., 2013, The study of beryl pegmatites of Ebrahim Attar and related skarn (southwest of Ghorveh), 23rd Symposium of Crystallography and Mineralogy of Iran, Damghan, p. 825–829. *(in Persian)*.

Salami, S., Sepahi, A.A., and Maanijou, M., 2014, Study of pegmatites from Ebrahim Attar and related skarns (southwest of Ghorveh): Iranian Journal of Petrology, 22, 309–322.

Samadi, R., Miller, N.R., Mirnejad, H., Harris, C., Kawabata, H., and Shirdashtzadeh, N., 2014, Origin of garnet in aplite and pegmatite from Khajeh Morad in northeastern Iran: A major, trace element, and oxygen isotope approach: Lithos, 208, 378–392. doi:10.1016/j.lithos.2014.08.023.

Samson, I.M., and Sinclair, W.D., 1992, Magmatic hydrothermal fluids and the origin of quartz-tourmaline orbicules in the

Seagull batholith, Yukon Territory: The Canadian Mineralogist, 30, 937–954.

Sepahi, A., Salami, S., Lentz, D., McFarlane, C., and Maanijou, M., 2018, Petrography, geochemistry, and U–Pb geochronology of pegmatites and aplites associated with the Alvand intrusive complex in the Hamedan region, Sanandaj–Sirjan zone, Zagros orogen (Iran): International Journal of Earth Sciences, 107, 1–38. doi:10.1007/s00531-017-1515-4.

Sepahi, A.A., 1999, Petrology of the Alvand plutonic complex with special reference on granitoids [Ph.D. thesis]: Tarbiat Moallem University of Tehran, 326 p.

Sepahi, A.A., 2007, A detailed study of morphology and chemistry of garnet crystals with suggestion of new subdivision: Data from pelitic schists, hornfelses and aplites of Hamedan region, Iran: Iranian Journal of Science and Technology, Transaction, 31, 281–289.

Sepahi, A.A., and Athari, S.F., 2006, Petrology of major granitic plutons of the northwestern part of the Sanandaj-Sirjan Metamorphic Belt, Zagros Orogen, Iran, with emphasis on A-type granitoids from the SE Saqqez area: Neues Jahrbuch für Mineralogie-Abhandlungen: Journal of Mineralogy and Geochemistry, 183, 93–106. doi:10.1127/0077-7757/2006/0063.

Sepahi, A.A., Shahbazi, H., Siebel, W., and Ranin, A., 2014, Geochronology of plutonic rocks from the Sanandaj-Sirjan zone, Iran and new zircon and titanite U-Th-Pb ages for granitoids from the Marivan pluton: Geochronometria, 41, 207–215. doi:10.2478/s13386-013-0156-z.

Shabanian, N., Davoudian, A.R., Dong, Y., and Liu, X., 2017, U-Pb zircon dating, geochemistry and Sr-Nd-Pb isotopic ratios from Azna-Dorud Cadomian metagranites, Sanandaj-Sirjan Zone of Western Iran: Precambrian Research, 306, 41–60. doi:10.1016/j.precamres.2017.12.037.

Shahbazi, H., Salami, S., and Siebel, W., 2014, Genetic classification of magmatic rocks from the Alvand plutonic complex, Hamedan, western Iran, based on zircon crystal morphology: Chemie der Erde-Geochemistry, 74, 577–584. doi:10.1016/j.chemer.2013.11.001.

Shahbazi, H., Siebel, W., Pourmoafee, M., Ghorbani, M., Sepahi, A.A., Shang, C.K., and Abedini, M.V., 2010, Geochemistry and U–Pb zircon geochronology of the Alvand plutonic complex in Sanandaj–Sirjan Zone (Iran): New evidence for Jurassic magmatism: Journal of Asian Earth Sciences, 39, 668–683. doi:10.1016/j.jseaes.2010.04.014.

Shakerardakani, F., Neubauer, F., Masoudi, F., Mehrabi, B., Liu, X., Dong, Y., Mohajjel, M., Monfaredi, B., and Friedl, G., 2015, Panafrican basement and Mesozoic gabbro in the Zagros orogenic belt in the Dorud–Azna region (NW Iran): Laser-ablation ICP–MS zircon ages and geochemistry: Tectonophysics, 647, 146–171. doi:10.1016/j.tecto.2015.02.020.

Sheikhi, F., Alaminia, Z., and Tabakh Shabani, A.A., 2012, Seranjic skarn geothermometery (SW Ghorveh, Kordestan Province): Iranian Journal of Crystallography and Mineralogy, 20, 343–354. *(in Persian)*.

Shewfelt, D.A., 2005, The nature and origin of Western Australian tourmaline nodules; a petrologic, geochemical and Isotopic study [Ph.D. thesis]: University of Saskatchewan.

Sinclair, W.D., and Richardson, J.M., 1992, Quartz-tourmaline orbicules in the Seagull batholith, Yukon Territory: The Canadian Mineralogist, 30, 923–935.

Smith, H.J., Spivack, A.J., Staudigel, H., and Hart, S. R., 1995, The boron isotopic composition of altered oceanic crust: Chemical Geology, v. 126, p. 119 –135. doi: 10.1016/0009-2541(95)00113-6.

Somarin, A.K., 2004, Marano volcanic rocks, east Azerbaijan province, Iran, and associated Fe mineralization: Journal of Asian Earth Sciences, 24, 11–23. doi:10.1016/S1367-9120(03)00152-4.

Stöcklin, J., 1968, Structural history and tectonics of Iran: A review: American Association of Petroleum Geologists, 52, 1229–1258.

Tabbakh Shabani, A., Zarei Sahamieh, R., and Keshavarz, Z., 2013, Composition of Tourmalines from Hajiabad and Dehgah area: SE Boroujerd: Geopersia, 3, 21–33. doi:10.22059/jgeope.2013.36012.

Tahmasbi, Z., 2014, The formation mechanism of tourmaline nodules in Boroujerd area (Dehgah-Sarsakhti): Iranian Journal of Crystallography and Mineralogy, 22, 419–430. doi: ijcm.ir/article-1-224-fa.html. *(in Persian)*.

Tahmasbi, Z., Ahmadi Khalaji, A., and Rajaeieh, M., 2009, Tourmalinization in the Astaneh granitoids (south west Arak): Iranian Journal of Crystallography and Mineralogy, 17, 369–380. ijcm.ir/article-1-567-fa.html. *(in Persian)*. .

Tahmasbi, Z., Castro, A., Khalili, M., Khalaji, A.A., and de la Rosa, J., 2010, Petrologic and geochemical constraints on the origin of Astaneh pluton, Zagros orogenic belt, Iran: Journal of Asian Earth Sciences, 39, 81–96. doi:10.1016/j.jseaes.2010.03.001.

Tahmasbi, Z., Zal, F., and Khalaji, A.A., 2017, Geochemistry and formation of tourmaline nodules in Mashhad leucogranite, Iran: Geosciences Journal, 21, 341–353. doi:10.1007/s12303-016-0027-8.

Tkachev, A.V., 2011, Evolution of metallogeny of granitic pegmatites associated with orogens throughout geological time: Geological Society: London, Special Publications, Vol. 350, 7–23. doi:10.1144/SP350.2.

Trumbull, R.B., Krienitz, M.-S., Gottesmann, B., and Wiedenbeck, M., 2008, Chemical and boron-isotope variations in tourmalines from an S-type granite and its source rocks: The Erongo granite and tourmalinites in the Damara Belt, Namibia: Contributions to Mineralogy and Petrology, 155, 1–18. doi:10.1007/s00410-007-0227-3.

Valizadeh, M.V., and Torkian, A., 1999, The Study of petrography and petrology of pegmatites in the Hamadan area: Journal of Science, University of Tehran, 25, 121–135.

Van Hinsberg, V.J., Henry, D.J., and Marschall, H.R., 2011, Tourmaline: An ideal indicator of its host environment: The Canadian Mineralogist, 49, 1–16. doi:10.3749/canmin.49.1.1.

Veksler, I.V., 2004, Liquid immiscibility and its role at the magmatic–Hydrothermal transition: A summary of experimental studies: Chemical Geology, 210, 7–31. doi:10.1016/j.chemgeo.2004.06.002.

Veksler, I.V., and Thomas, R., 2002, An experimental study of B-, P-and F-rich synthetic granite pegmatite at 0.1 and 0.2 GPa: Contributions to Mineralogy and Petrology, 143, 673–683. doi:10.1007/s00410-002-0368-3.

Wang, R.C., Che, X.D., Zhang, W.L., Zhang, A.C., and Zhang, H., 2009, Geochemical evolution and late re-equilibration of Na–Cs-rich beryl from the Koktokay# 3 pegmatite (Altai, NW China): European Journal of Mineralogy, 21, 795–809. doi:10.1127/0935-1221/2009/0021-1936.

Weinberg, R.F., and Hasalová, P., 2015, Water-fluxed melting of the continental crust, A review: Lithos, 212, 158–188. doi:10.1016/j.lithos.2014.08.021.

Whitney, D.L., and Evans, B.W., 2010, Abbreviations for names of rock forming minerals: American Mineralogist, 95, 185–187. doi:10.2138/am.2010.3371.

Whitworth, M.P., 1992, Petrogenetic implications of garnets associated with lithium pegmatites from SE Ireland: Mineralogical Magazine, 56, 75–83. doi:10.1180/minmag.1992.056.382.10.

Wood, S.A., 1992, Theoretical prediction of speciation and solubility of beryllium in hydrothermal solution to 300 C at saturated vapor pressure: Application to bertrandite/phenakite deposits: Ore Geology Reviews, 7, 249–278. doi:10.1016/0169-1368(92)90012-A.

Worden, R.H., Smalley, P.C., and Cross, M.M., 2000, The influence of rock fabric and mineralogy on thermochemical sulfate reduction: Khuff Formation: Abu Dhabi: Journal of Sedimentary Research, 70, 1210–1221. doi:10.1306/110499701210.

Yajam, S., Ghalamghash, J., Montero, P., Scarrow, J.H., Razavi, S.M.H., and Bea, F., 2015, The spatial and compositional evolution of the Late Jurassic Ghorveh-Dehgolan plutons of the Zagros Orogen, Iran: Geologica acta, 13, 25–43. doi:10.1344/GeologicaActa2015.13.1.2.

Zhang, H., Chen, J., Yang, T., Hou, Z., and Aghazadeh, M., 2018, Jurassic granitoids in the northwestern Sanandaj–Sirjan zone: Evolving magmatism in response to the development of a neo-Tethyan slab window: Gondwana Research, doi:10.1016/j.gr.2018.01.012.

Zhou, T., Yuan, F., Yue, S., Liu, X., Zhang, X., and Fan, Y., 2007, Geochemistry and evolution of ore-forming fluids of the Yueshan Cu–Au skarn-and vein-type deposits, Anhui Province, South China: Ore Geology Reviews, 31, 279–303. doi:10.1016/j.oregeorev.2005.03.016.